Credits: Geoff Chen

Building the SPT-3G 2019/2020 likelihood

Etienne Camphuis (IAP)

with Silvia Galli, Karim Benabed and Eric Hivon

Colloque national CMB-France #4 - November 23rd, 2022

Outline

A. **Overview of SPT-3G 2019/2020**

B. High precision inpainting of the SPT-3G data

South Pole Telescope

Details

- 10-meter diameter telescope located at the South Pole in optimal conditions for microwave observations, observing CMB anisotropies
- SPT-3G: state-of-the art instrument with 3 frequencies 90, 150, 220 GHz
- Beam: 1.6'/1.2'/1.0' (*Planck*: 5')
- Final map depth: 2.8, 2.6, 6.6 μK-arcmin (T) vs *Planck* 40 μK-arcmin
- See Sobrin et al. 2022 for more details

SPT

Credits: A. Chohski

SPT-3G baseline field

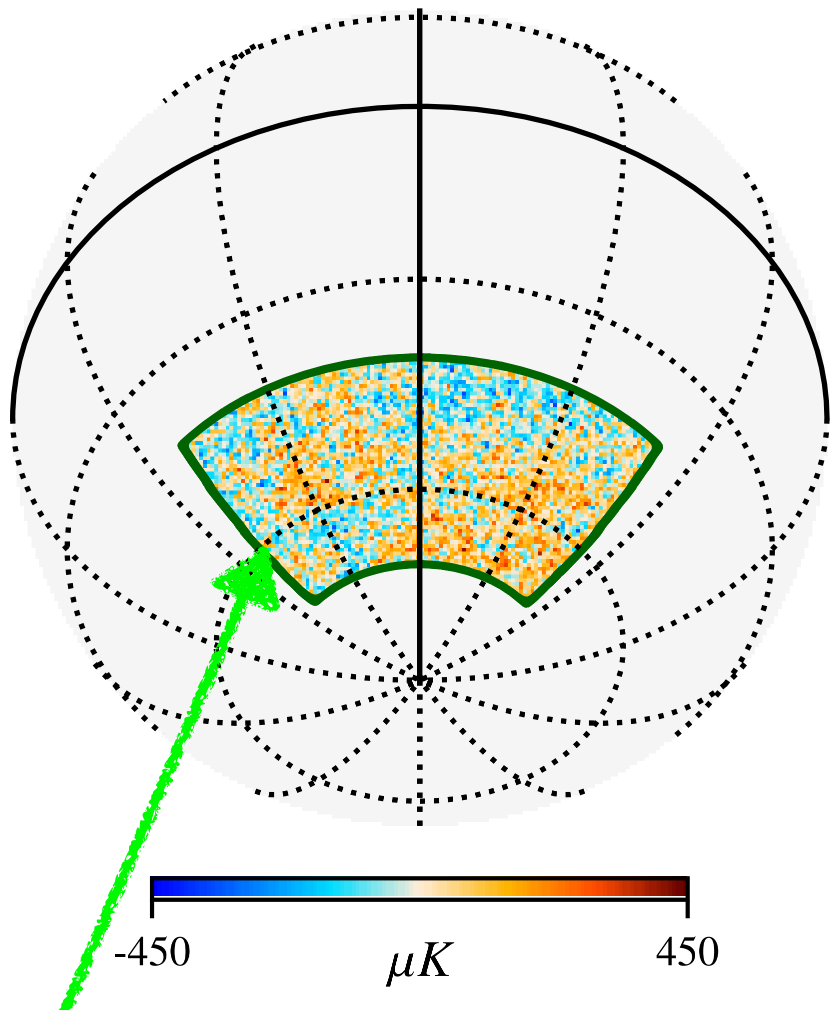

Data: T, Q, U maps

Credits: F. Guidi

South Pole Telescope

Forecasts

- 10-meter diameter telescope located at the South Pole in optimal conditions for microwave observations, observing CMB anisotropies
- SPT-3G: state-of-the art instrument with 3 frequencies 90, 150, 220 GHz
- Beam: 1.6’/1.2’/1.0’ (*Planck*: 5’)
- Final map depth: 2.8, 2.6, 6.6 μK-arcmin (T) vs *Planck* 40 μK-arcmin
- See <u>Sobrin et al. 2022</u> for more details

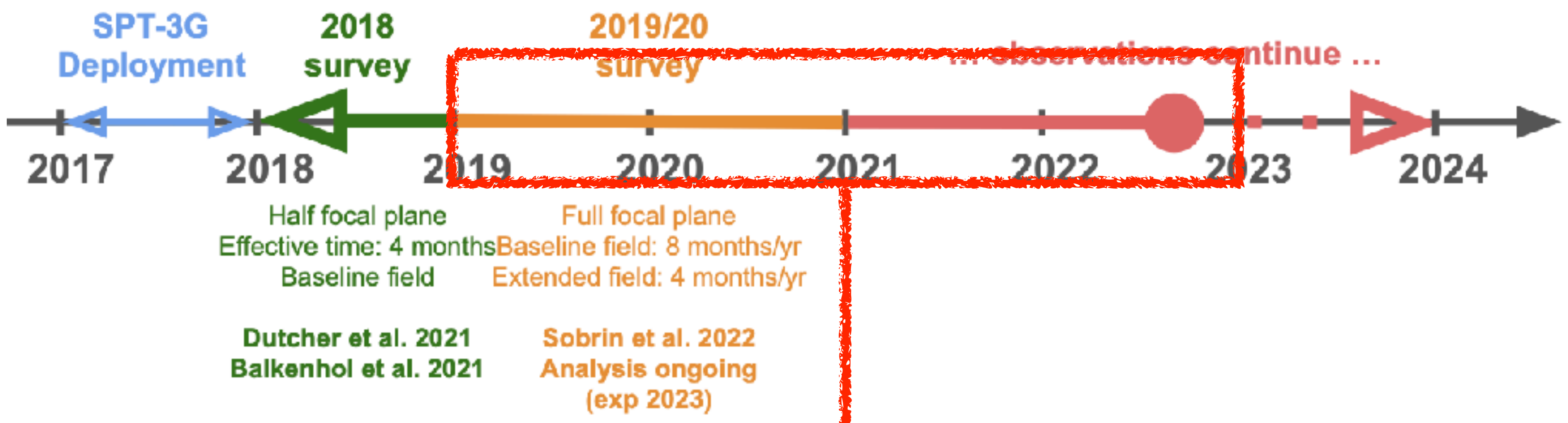

Forecasts on ΛCDM parameters with SPT-3G (5 years) data

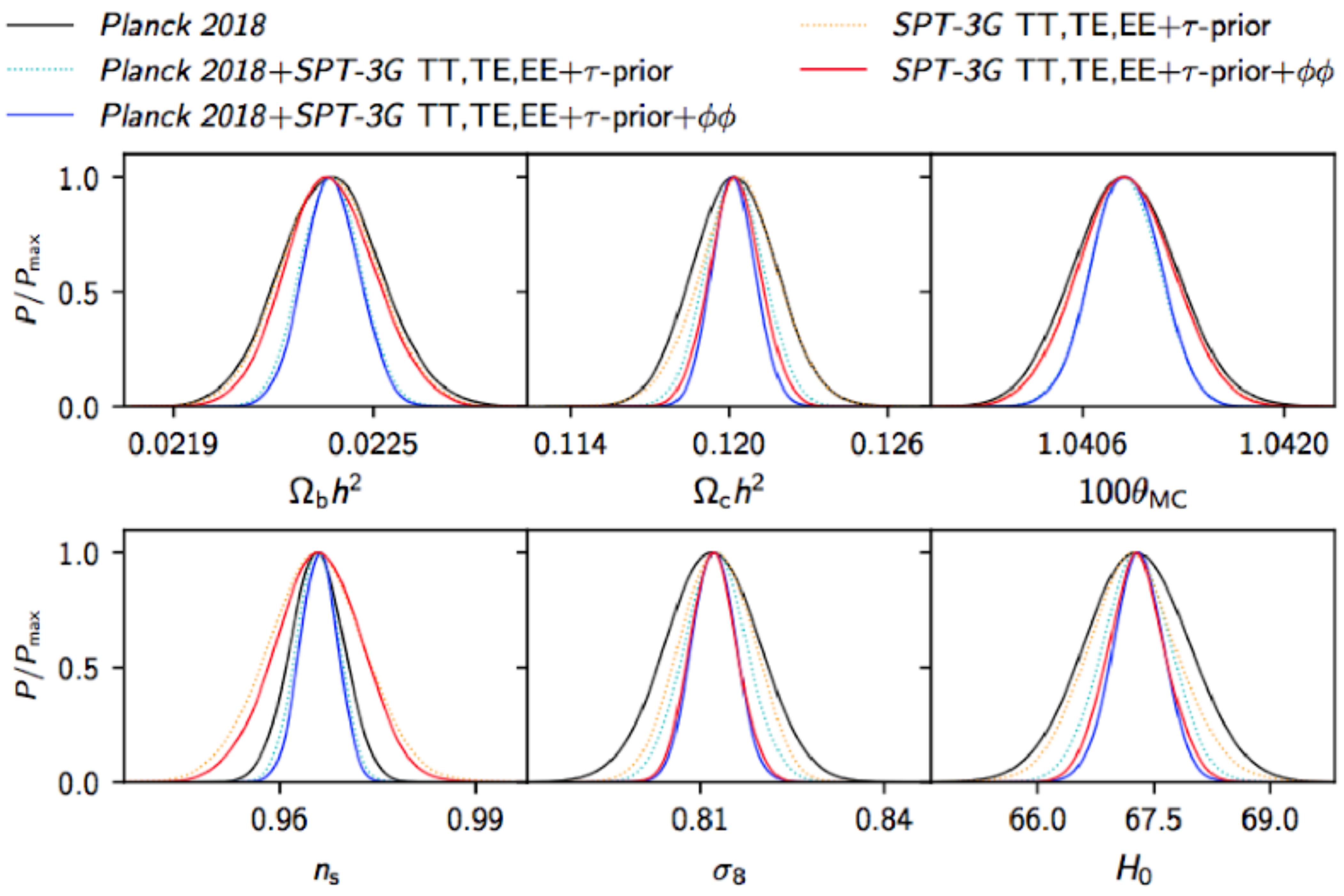

Credits: Silvia Galli

Outline

A. Overview of SPT-3G 2019/2020

B. High precision inpainting of the SPT-3G data

Analytical covariance

- For SPT-3G 2018, mock-observations are used to build the covariance matrix of the data vector of primary anisotropies (TTTEEE) => we replace it by a precise and fast analytical computation of the covariance developed in [Camphuis et al. 2022]

Power spectrum gaussian likelihood :

$$-\ln \mathscr{L}(\hat{C}\,|\,\Lambda\mathrm{CDM})$$

$$\propto \frac{1}{2}(\hat{C} - C^{\mathrm{th}})^T \boxed{\Sigma^{-1}} (\hat{C} - C^{\mathrm{th}}))$$

Analytical covariance

- For SPT-3G 2018, mock-observations are used to build the covariance matrix of the data vector of primary anisotropies (TTTEEE) => we replace it by a precise and fast analytical computation of the covariance developed in [Camphuis et al. 2022]

- **The mask W is a key ingredient of the covariance**

Power spectrum gaussian likelihood :

$$-\ln \mathscr{L}(\hat{C}\,|\,\Lambda\mathrm{CDM}) \propto \frac{1}{2}(\hat{C} - C^{\mathrm{th}})^T \boxed{\Sigma^{-1}}(\hat{C} - \boxed{C^{\mathrm{th}}})$$

Fiducial power spectrum

$$\mathrm{Cov}(\hat{C}_\ell, \hat{C}_{\ell'}) = 2\Xi_{\ell\ell'}[\boxed{W^2}] \sum_{\ell_1\ell_2} \boxed{C^{\mathrm{th}}_{\ell_1}}\, \bar{\Theta}^{\ell_1\ell_2}_{\ell\ell'}[\boxed{W}]\; C^{\mathrm{th}}_{\ell_2}$$

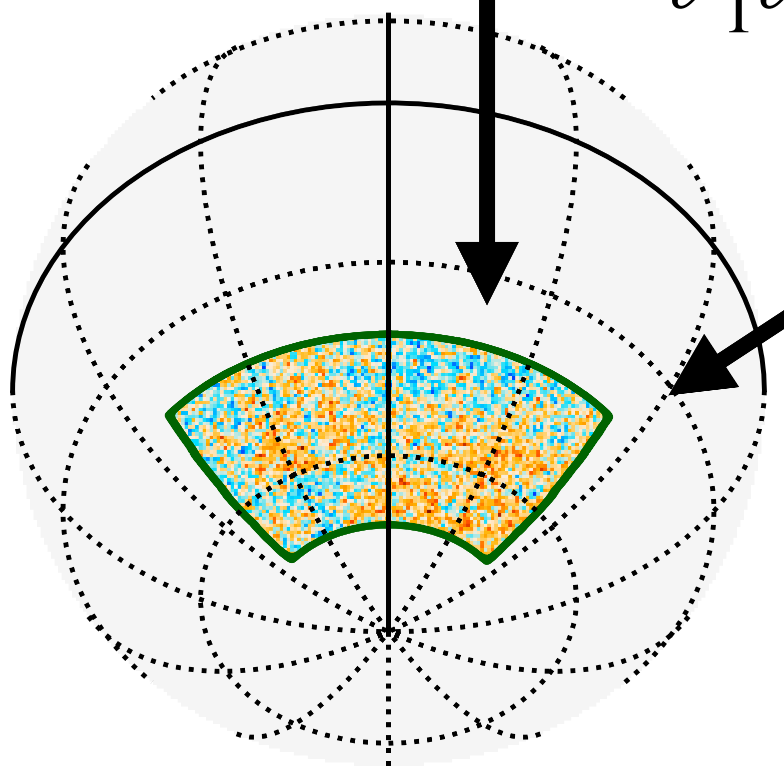

Baseline « winter » field

Effect of the mask

σ: correlation matrix

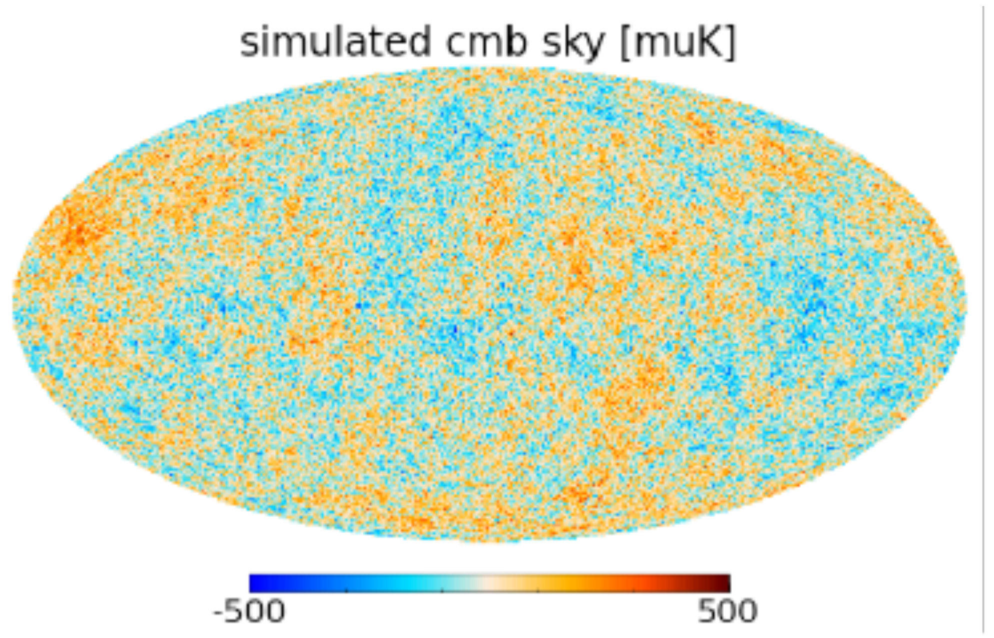

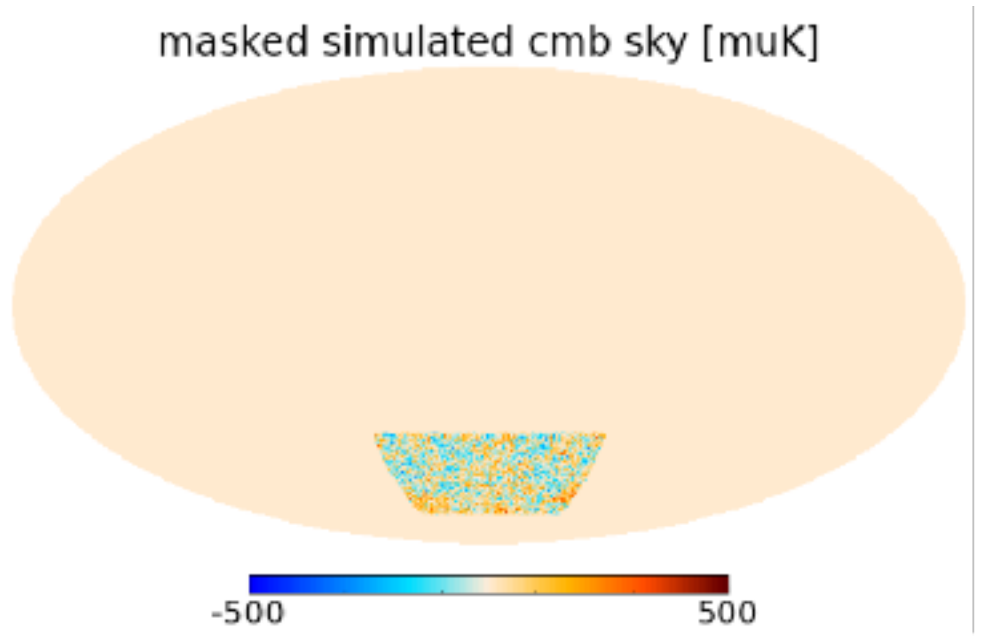

Analytical approximation of the covariance **works**

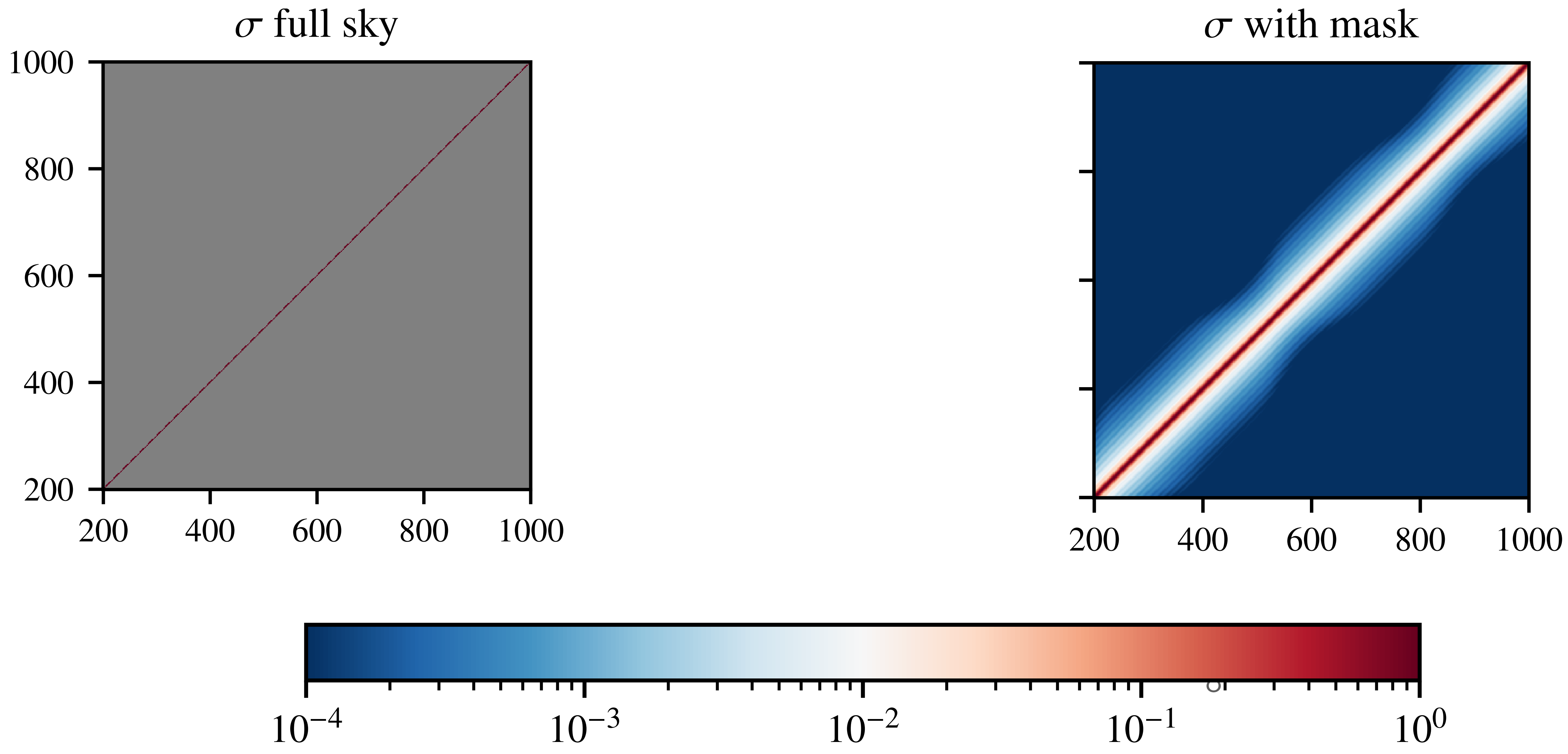

Effect of the mask

σ: correlation matrix

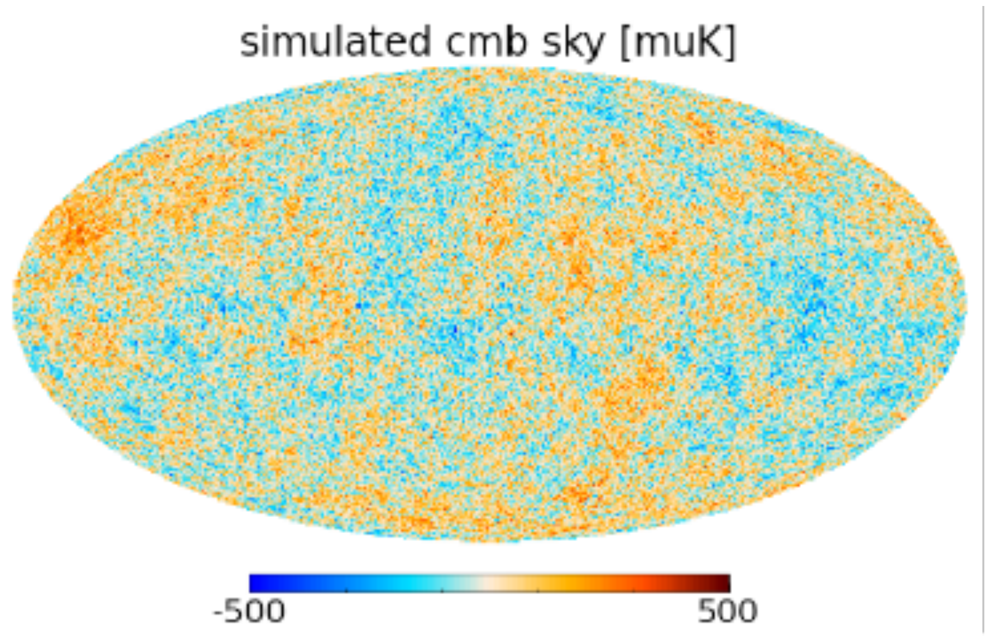

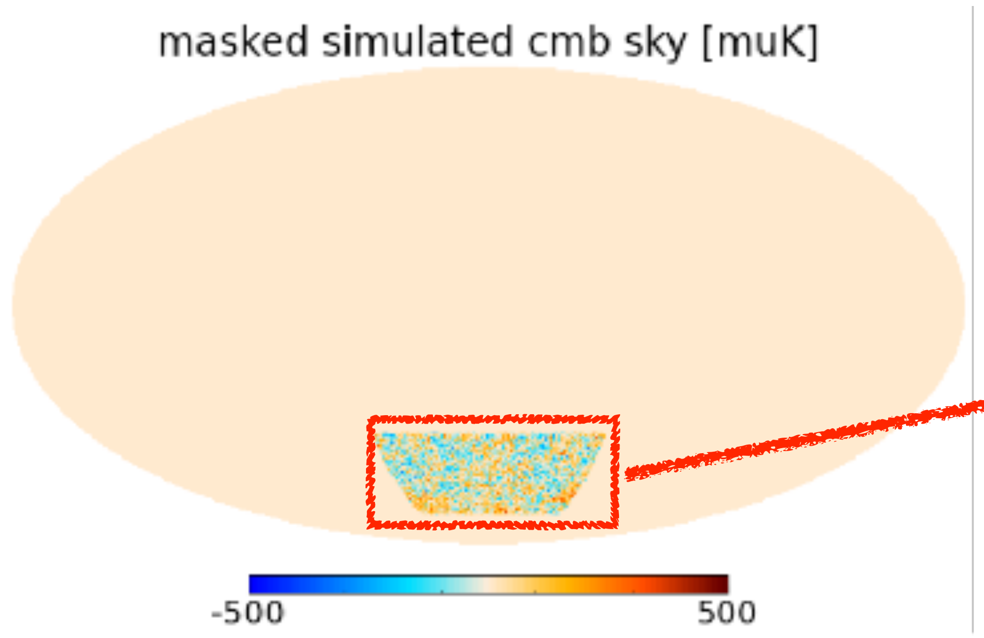

We must mask sources

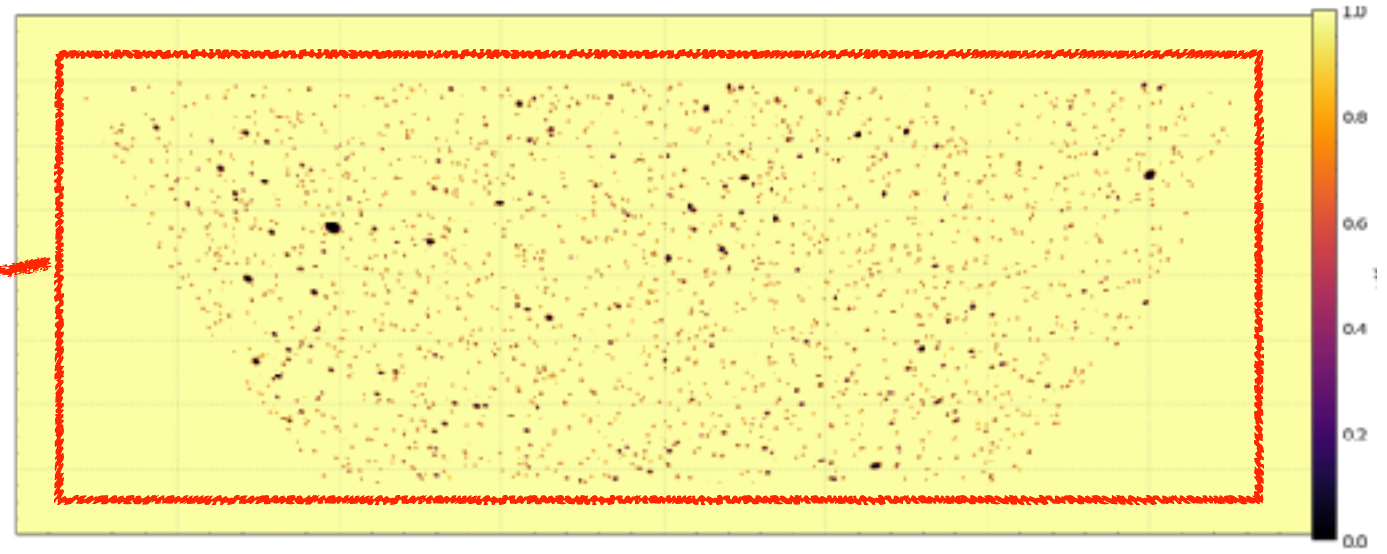

Analytical approximation of the covariance **works**

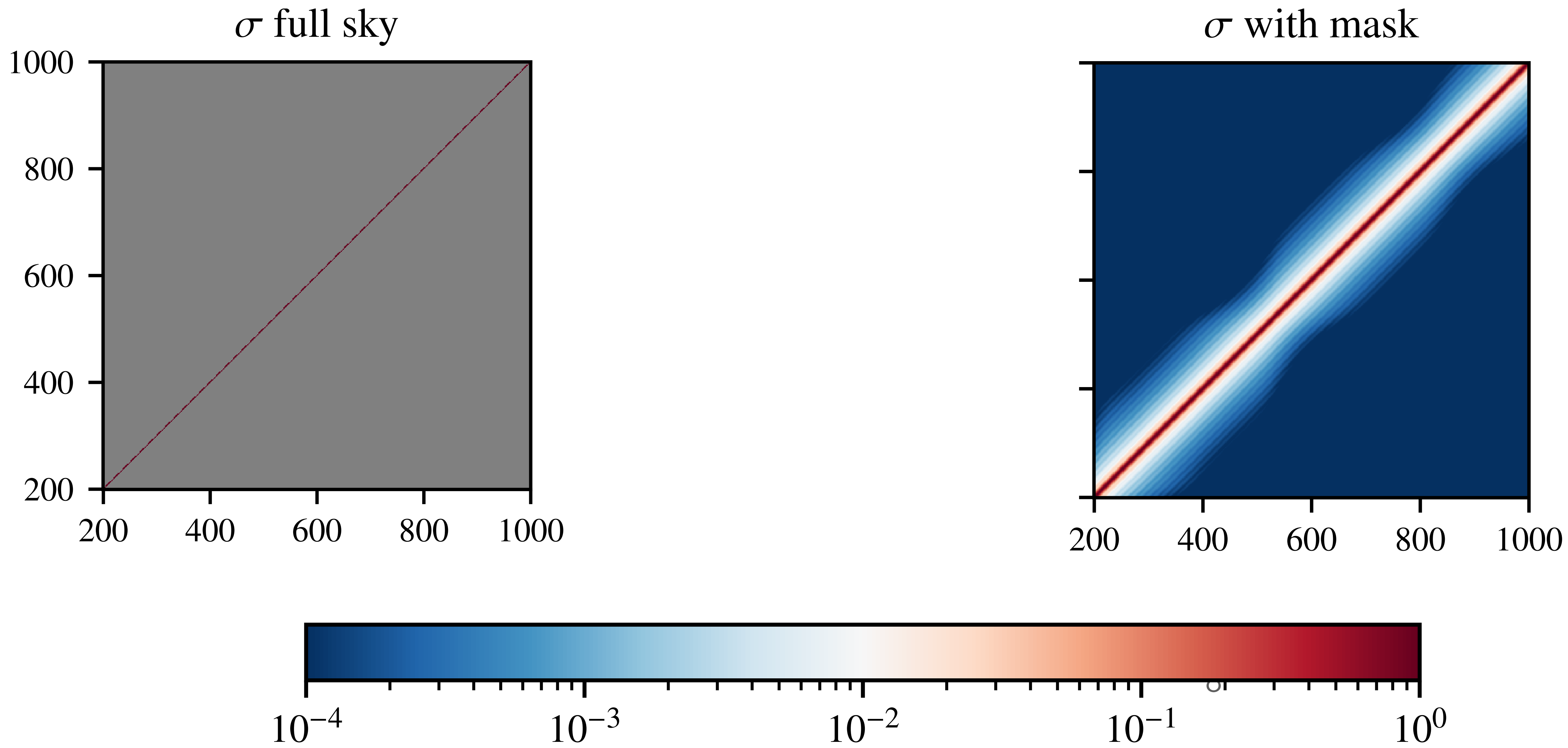

Analytical approximation of the covariance **fails** because it does not model correctly the additional coupling and additional variance

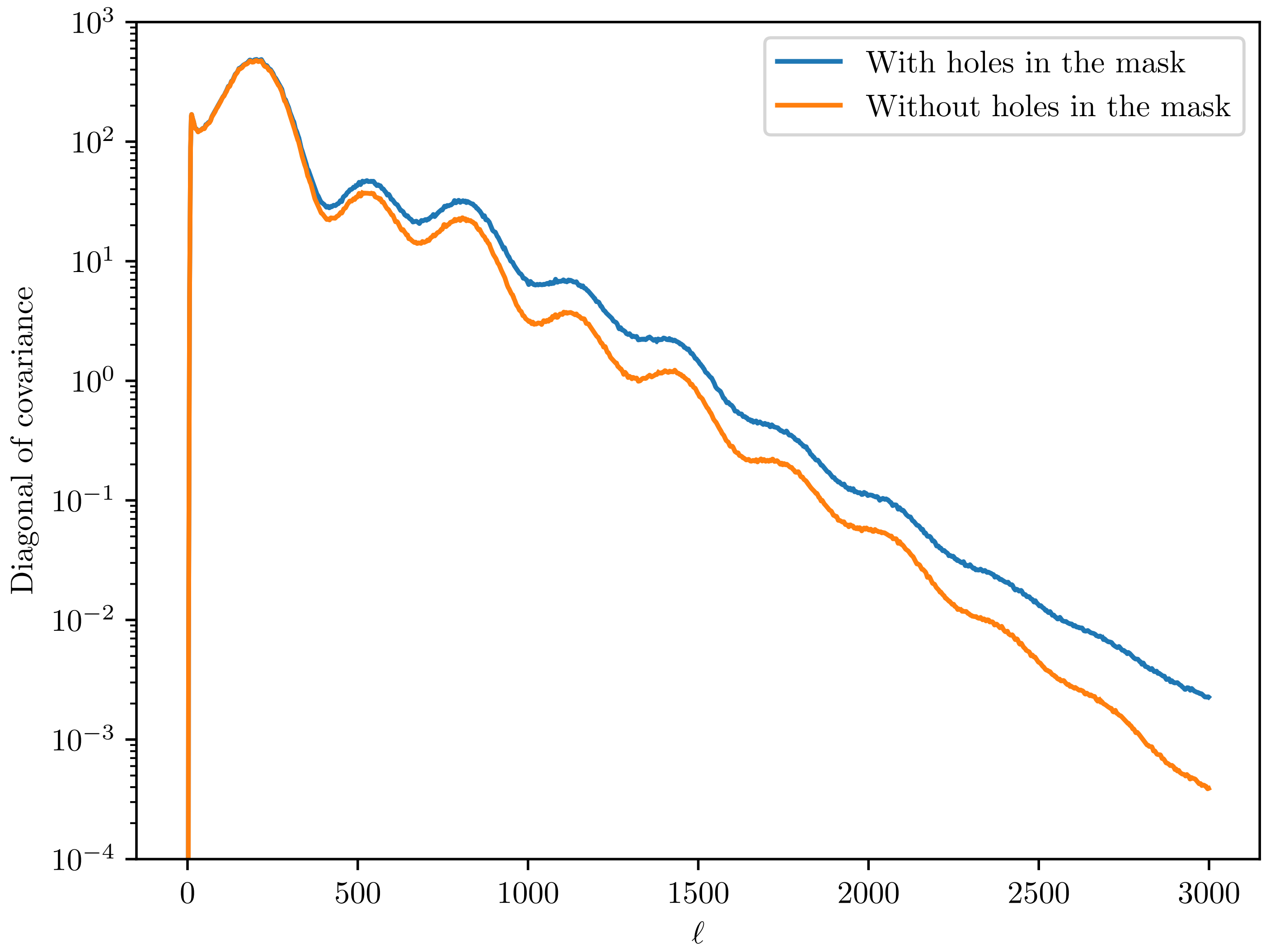

Effect of the mask - source masking

We can not use our analytical approximation of the covariance

Mask with holes: simulations vs analytical approximation
diagonals

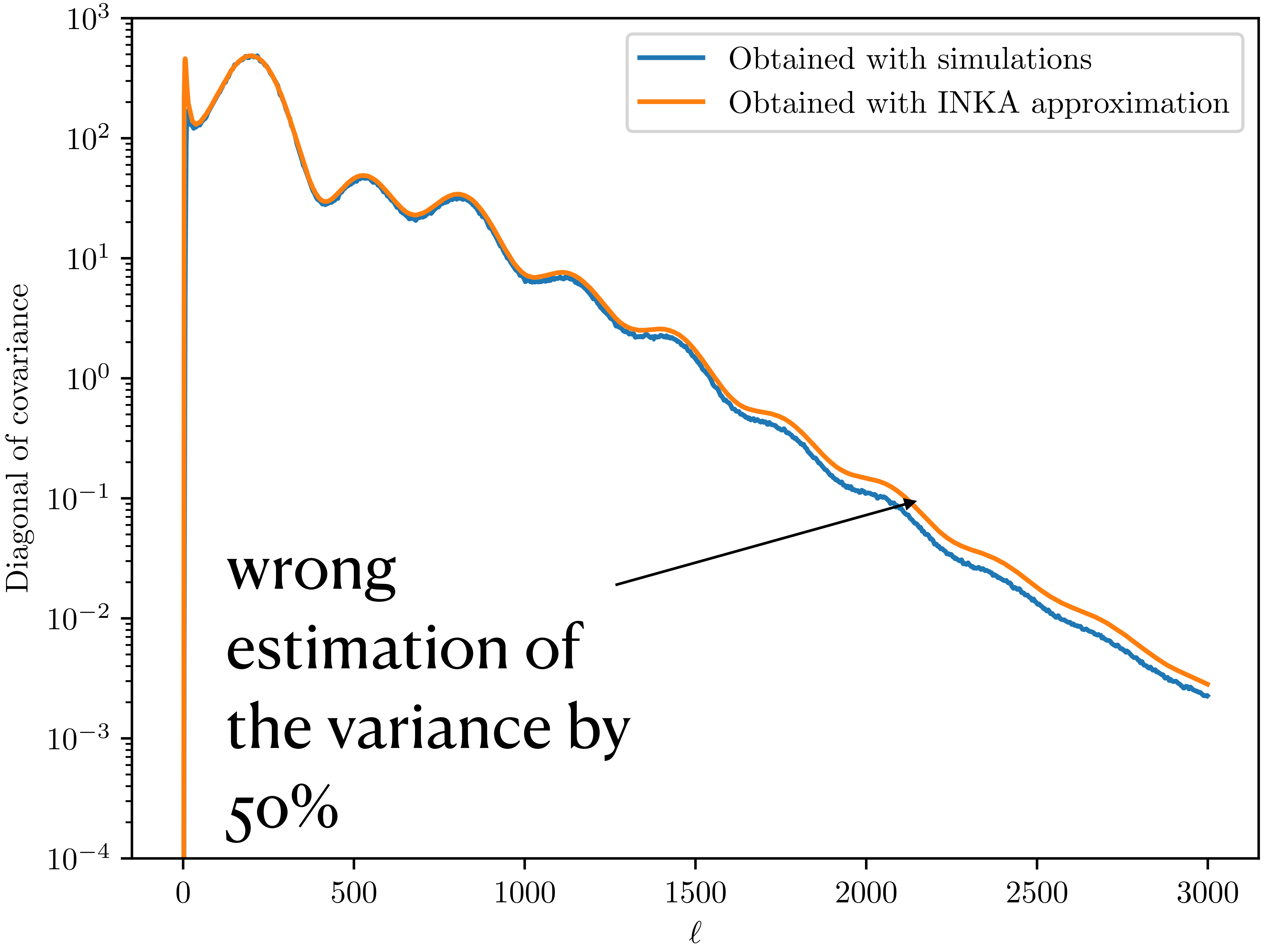

Mask with holes: simulations vs analytical approximation
rank of correlation

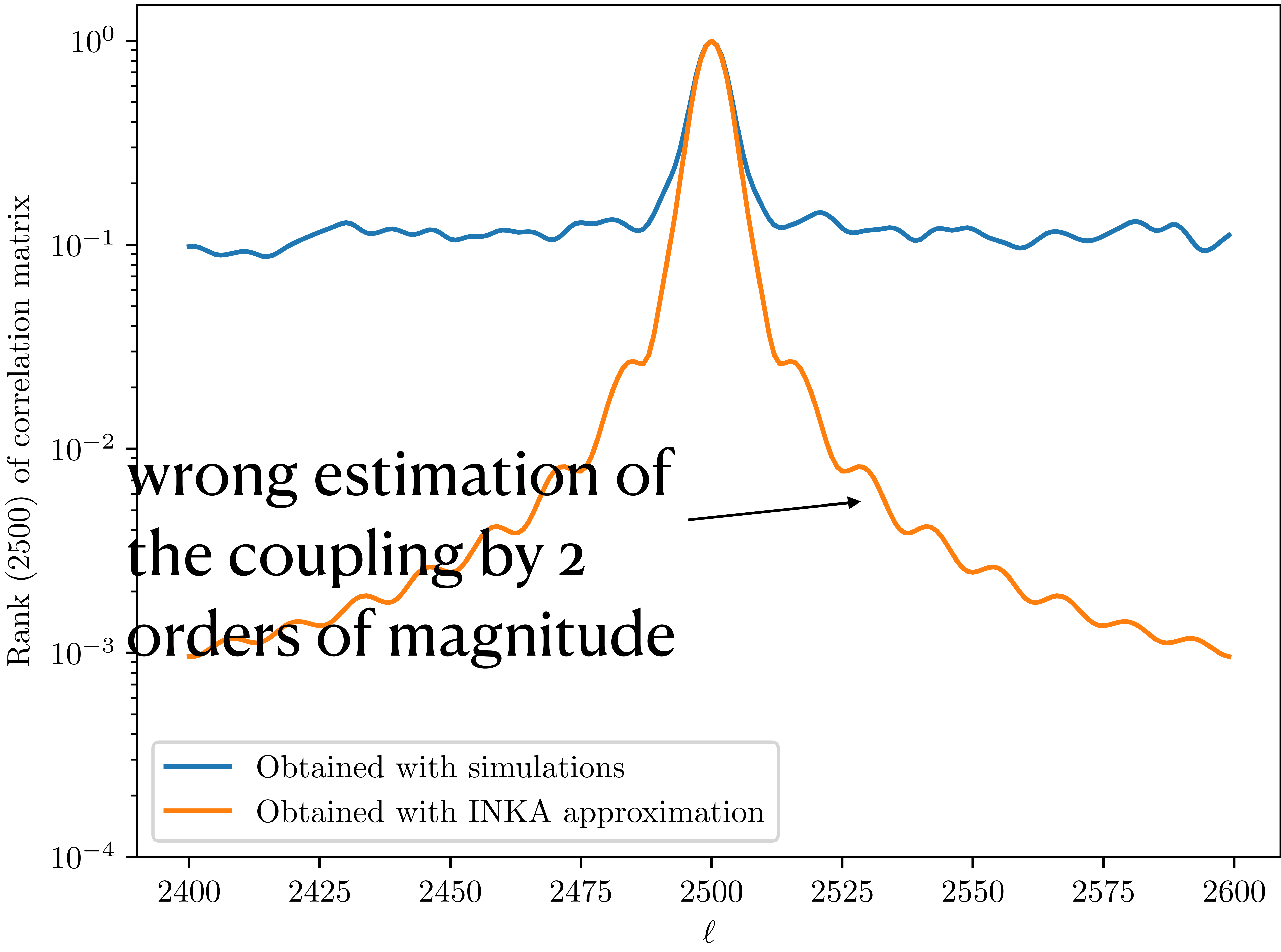

Our solution: inpainting

- Gaussian constrained realization of the CMB anisotropies:
$$\begin{pmatrix} T^{\mathrm{inp}} \\ Q^{\mathrm{inp}} \\ U^{\mathrm{inp}} \end{pmatrix} = X \begin{pmatrix} T^{\mathrm{data}} \\ Q^{\mathrm{data}} \\ U^{\mathrm{data}} \end{pmatrix} + (1 - X) \begin{pmatrix} T^{\mathrm{random}} \\ Q^{\mathrm{random}} \\ U^{\mathrm{random}} \end{pmatrix}$$

- Challenges: **high precision inpainting of high resolution maps with many sources** ($N_{\mathrm{sources}} \sim 2000$) **of varying radii.**

Our solution: inpainting

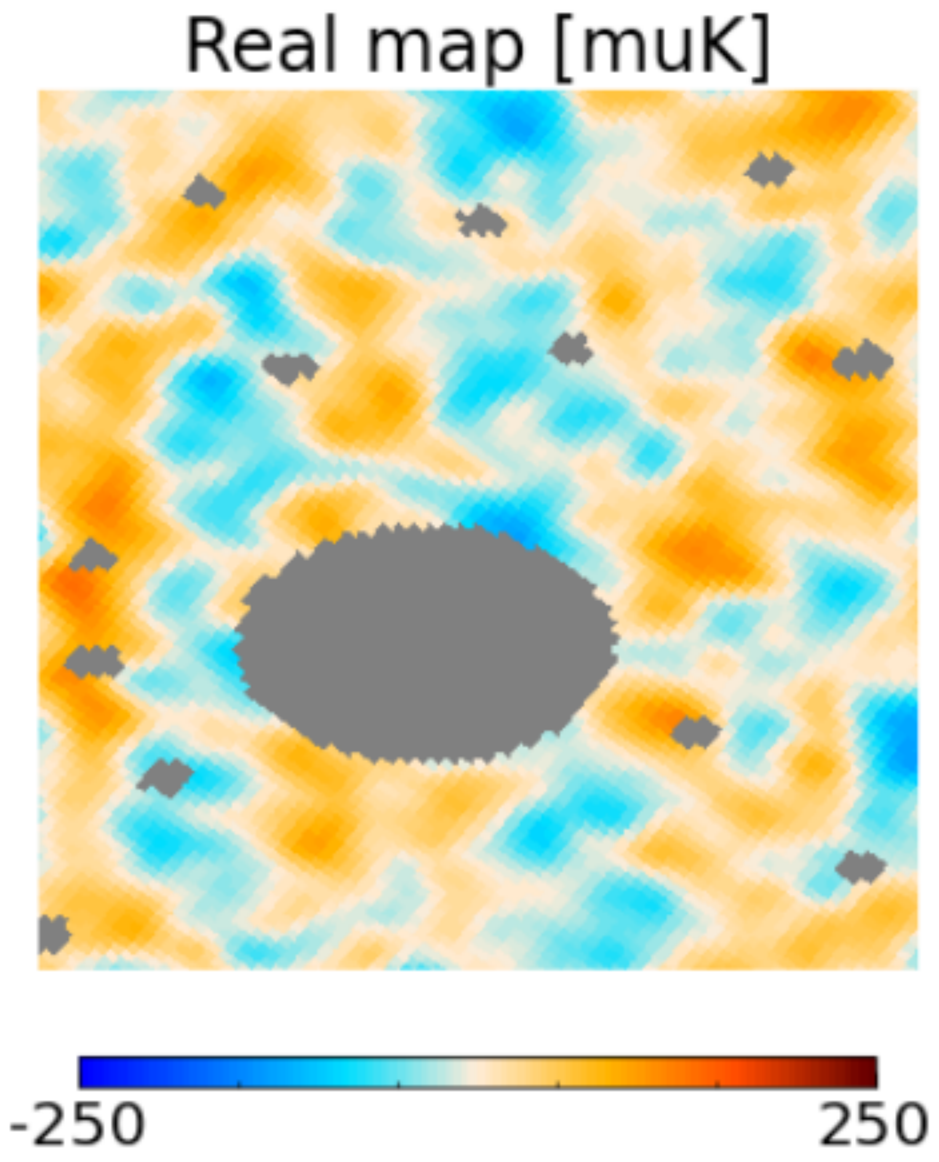

Data

- Gaussian constrained realization of the CMB anisotropies:

$$\begin{pmatrix} T^{\rm inp} \\ Q^{\rm inp} \\ U^{\rm inp} \end{pmatrix} = X \begin{pmatrix} T^{\rm data} \\ Q^{\rm data} \\ U^{\rm data} \end{pmatrix} + (1-X) \begin{pmatrix} T^{\rm random} \\ Q^{\rm random} \\ U^{\rm random} \end{pmatrix}$$

- Challenges: **high precision inpainting of high resolution maps with many sources** ($N_{\rm sources} \sim 2000$) **of varying radii.**

Our solution: inpainting

- Gaussian constrained realization of the CMB anisotropies:

$$\begin{pmatrix} T^{\rm inp} \\ Q^{\rm inp} \\ U^{\rm inp} \end{pmatrix} = X \begin{pmatrix} T^{\rm data} \\ Q^{\rm data} \\ U^{\rm data} \end{pmatrix} + (1 - X) \begin{pmatrix} T^{\rm random} \\ Q^{\rm random} \\ U^{\rm random} \end{pmatrix}$$

- Challenges: **high precision inpainting of high resolution maps with many sources ($N_{\rm sources} \sim 2000$) of varying radii.**

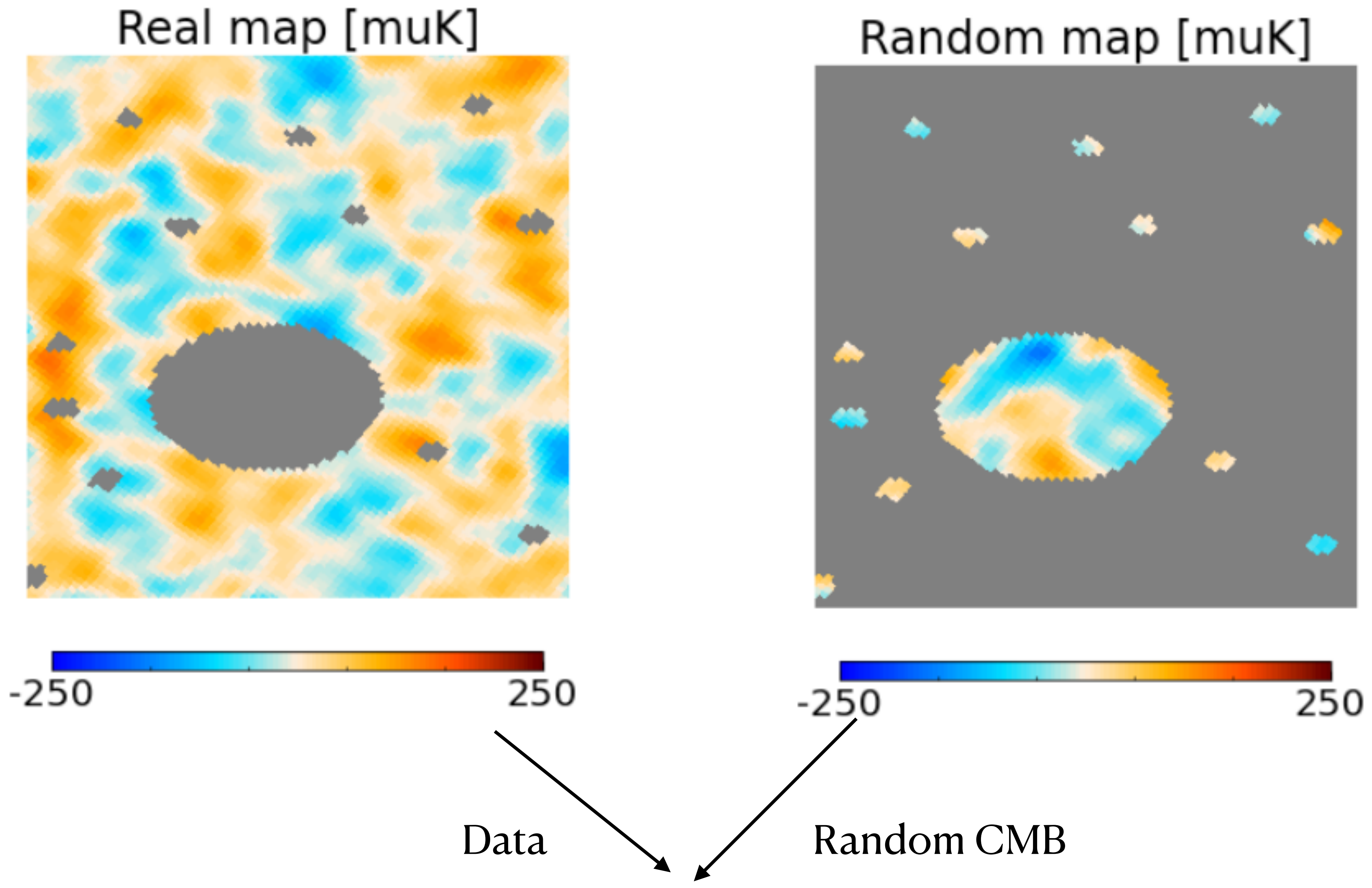

Our solution: inpainting

- Gaussian constrained realization of the CMB anisotropies:

$$\begin{pmatrix} T^{\mathrm{inp}} \\ Q^{\mathrm{inp}} \\ U^{\mathrm{inp}} \end{pmatrix} = \boxed{X} \begin{pmatrix} T^{\mathrm{data}} \\ Q^{\mathrm{data}} \\ U^{\mathrm{data}} \end{pmatrix} + (1 - \boxed{X}) \begin{pmatrix} T^{\mathrm{random}} \\ Q^{\mathrm{random}} \\ U^{\mathrm{random}} \end{pmatrix}$$

Optimal CMB reconstruction
Wiener filtering

- Challenges: **high precision inpainting of high resolution maps with many sources** ($N_{\mathrm{sources}} \sim 2000$) **of varying radii.**

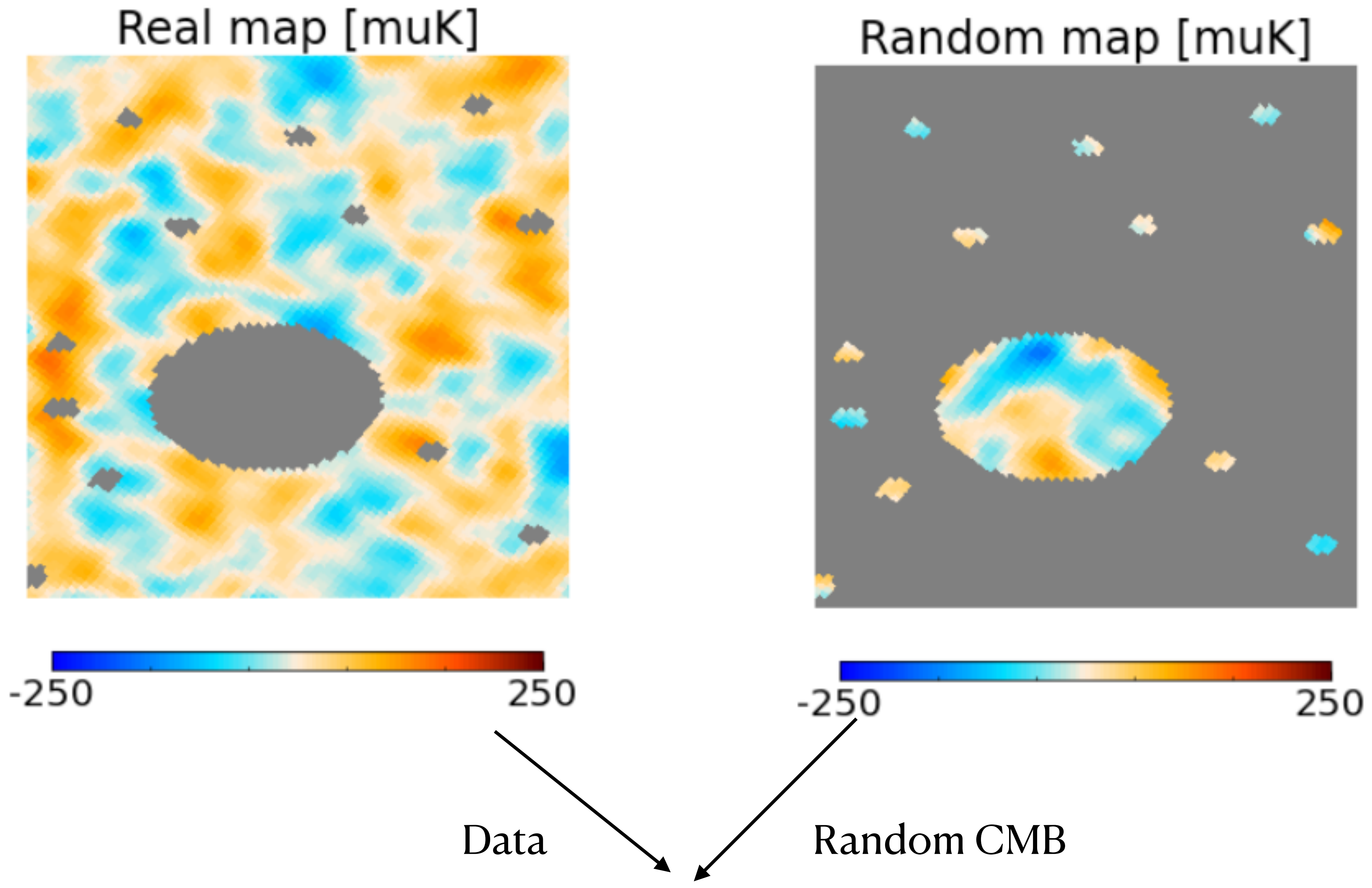

Our solution: inpainting

- Gaussian constrained realization of the CMB anisotropies:

$$\begin{pmatrix} T^{\rm inp} \\ Q^{\rm inp} \\ U^{\rm inp} \end{pmatrix} = \boxed{X} \begin{pmatrix} T^{\rm data} \\ Q^{\rm data} \\ U^{\rm data} \end{pmatrix} + (1 - \boxed{X}) \begin{pmatrix} T^{\rm random} \\ Q^{\rm random} \\ U^{\rm random} \end{pmatrix}$$

Optimal CMB reconstruction
Wiener filtering

- Challenges: **high precision inpainting of high resolution maps with many sources** ($N_{\rm sources} \sim 2000$) **of varying radii.**

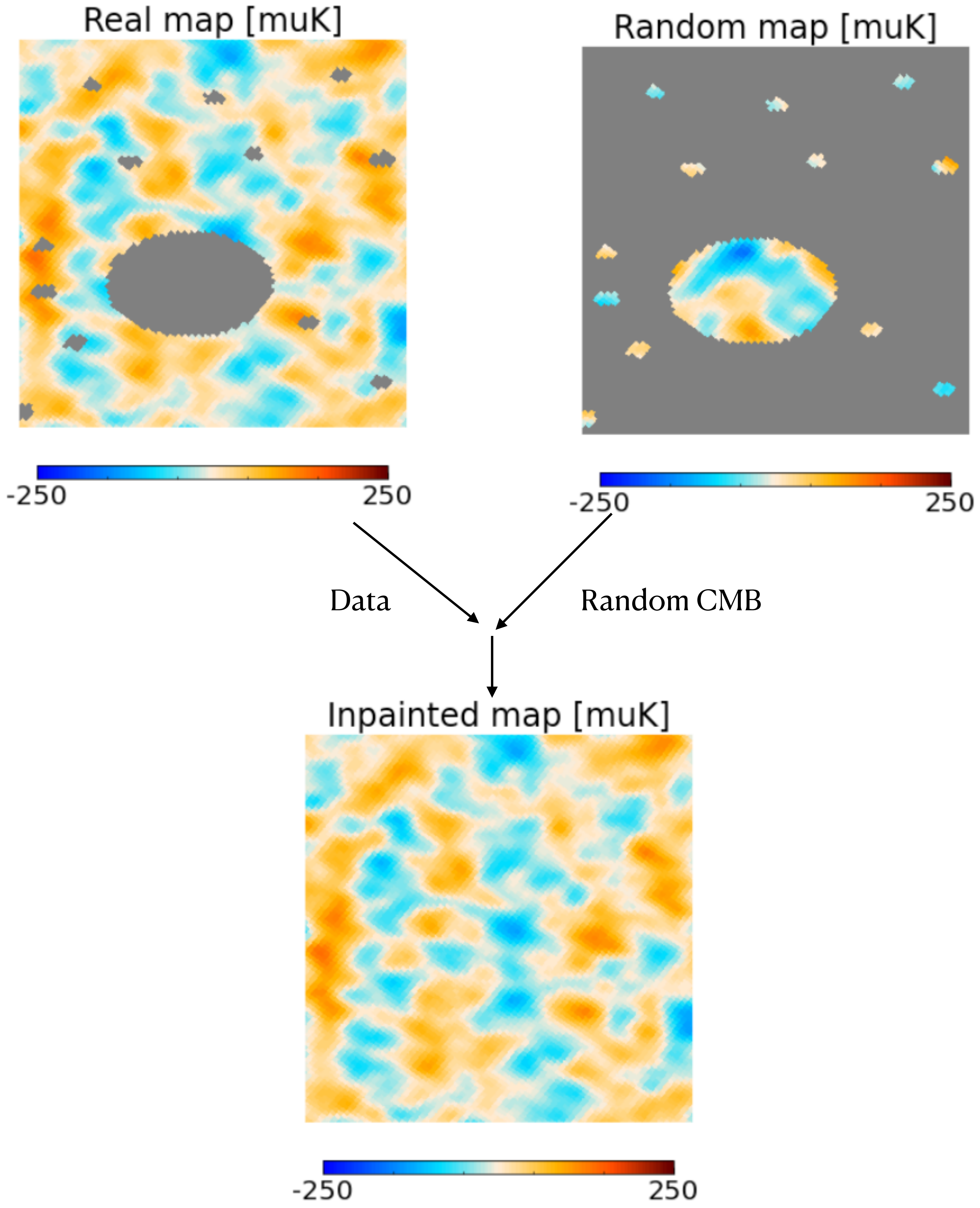

Our solution: inpainting

- Gaussian constrained realization of the CMB anisotropies

$$\underbrace{\begin{pmatrix} T^{\mathrm{inp}} \\ Q^{\mathrm{inp}} \\ U^{\mathrm{inp}} \end{pmatrix}}_{\text{Inpainted data}} = \underbrace{X \begin{pmatrix} T^{\mathrm{data}} \\ Q^{\mathrm{data}} \\ U^{\mathrm{data}} \end{pmatrix}}_{\text{Filtered data}} + \underbrace{(1 - X) \begin{pmatrix} T^{\mathrm{random}} \\ Q^{\mathrm{random}} \\ U^{\mathrm{random}} \end{pmatrix}}_{\text{Anti-filtered random realization}}$$

- $\langle \hat{C}_\ell^{\mathrm{inp}} \rangle = \langle \hat{C}_\ell^{XD} \rangle + \langle \hat{C}_\ell^{(1-X)R} \rangle = \langle \hat{C}_\ell^{\mathrm{data}} \rangle$
- Why adding a random CMB ? It allows to have an unbiased spectrum ! But inpainted CMB is **not** true CMB

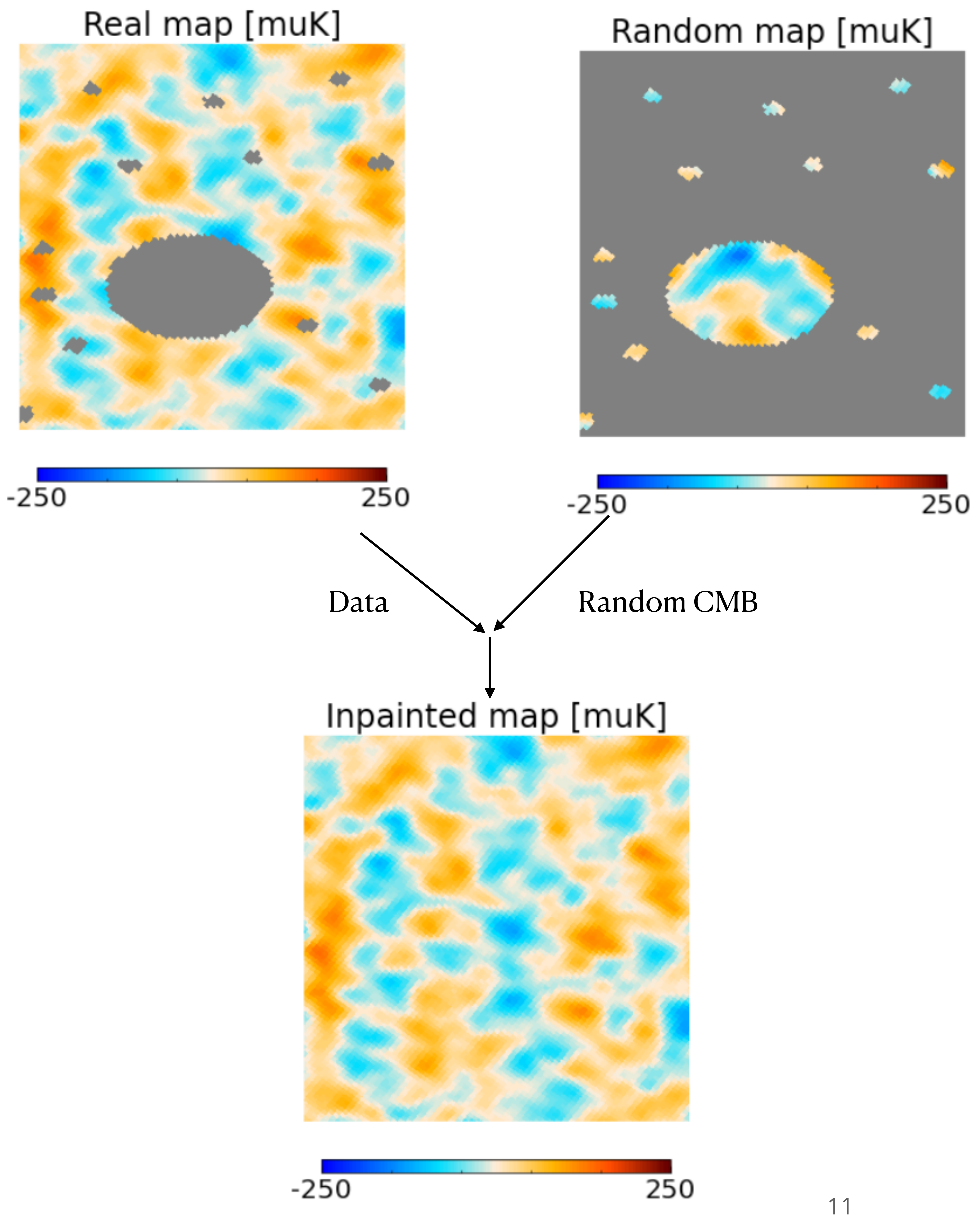

11

Our test pipeline

- In the following slides, I will show a series of tests asserting the validity of our method
- See pipeline to the right
- Plots will show the bias in units of cosmic deviation + noise
$$\frac{\langle \hat{C}_\ell^{\mathrm{inp}} \rangle - \langle \hat{C}_\ell^{\mathrm{bare}} \rangle}{\sigma\{C_\ell^{\mathrm{bare}}\}}$$
- I will show only temperature, but polarization (TE, EE) is similar

$$\begin{array}{ccccc} C_\ell^{\mathrm{fid}} & \rightarrow & T & \rightarrow & \hat{C}_\ell^{\mathrm{bare}} \\ & & \Big\downarrow{\scriptstyle \text{Inpainting}} & & \\ & & T^{\mathrm{inp}} & \rightarrow & \hat{C}_\ell^{\mathrm{inp}} \end{array}$$

1. High precision

- We restrict our inpainting to using nearby pixels for efficiency purpose
- We need to use a certain amount (more than 1 deg around the hole!) to reach high precision
- This corresponds to the size of the CMB correlation
- **We reach less that 5% of cosmic variance + noise error**

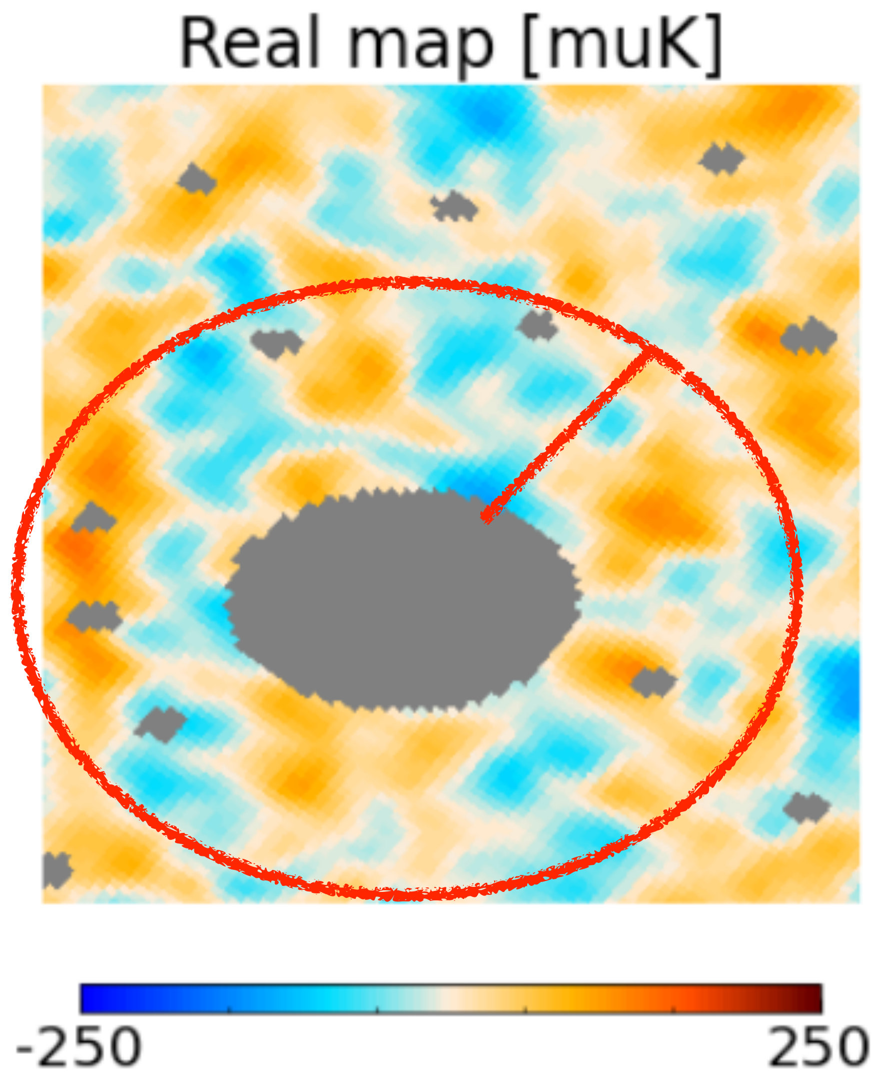

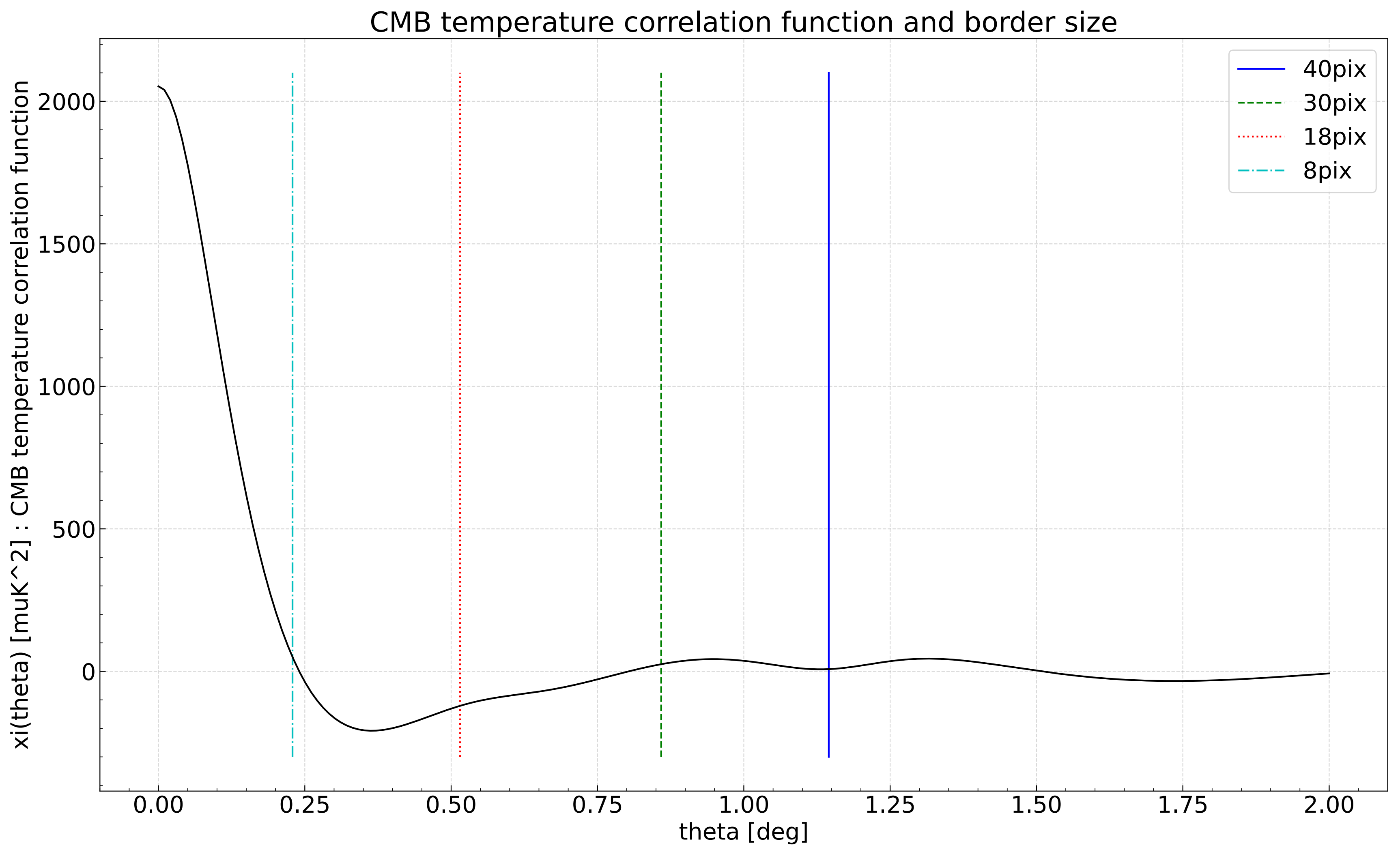

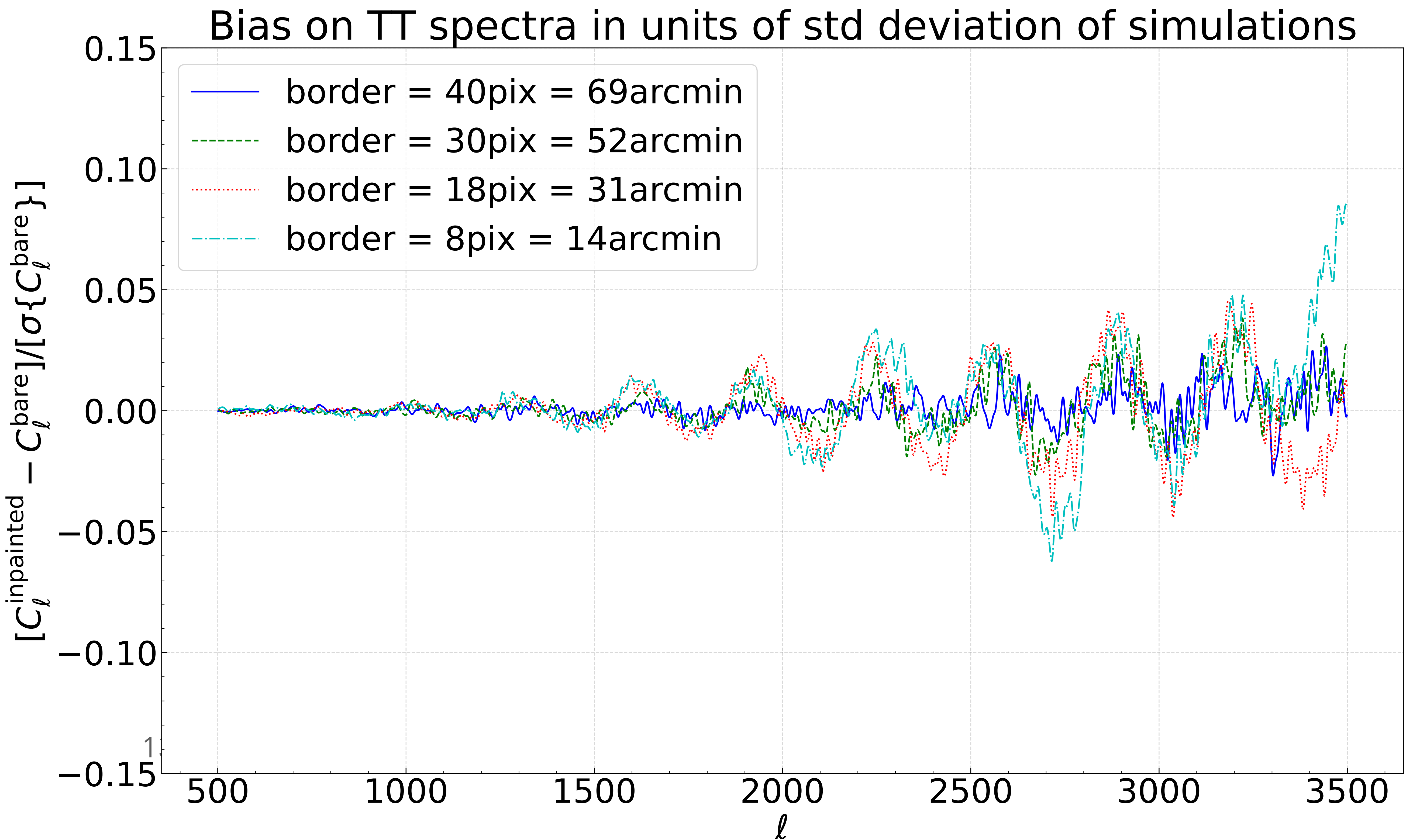

1. High precision

Temperature and polarization

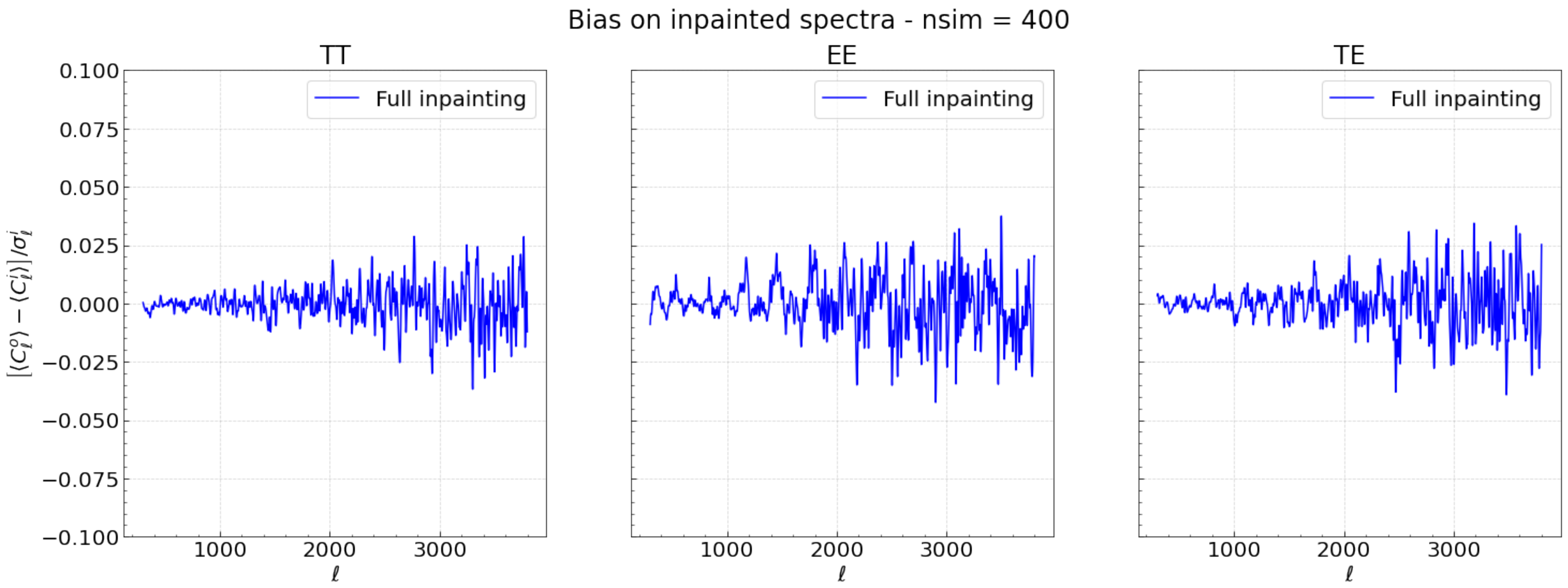

2. Robustness against input spectrum

$$\begin{pmatrix} T^{\mathrm{inp}} \\ Q^{\mathrm{inp}} \\ U^{\mathrm{inp}} \end{pmatrix} = \boxed{X} \begin{pmatrix} T^{\mathrm{data}} \\ Q^{\mathrm{data}} \\ U^{\mathrm{data}} \end{pmatrix} + (1 - \boxed{X}) \boxed{\begin{pmatrix} T^{\mathrm{random}} \\ Q^{\mathrm{random}} \\ U^{\mathrm{random}} \end{pmatrix}}$$

C_ℓ^{fid}

Inpainting requires a fiducial spectrum

We show that we are robust against variations of the input spectrum

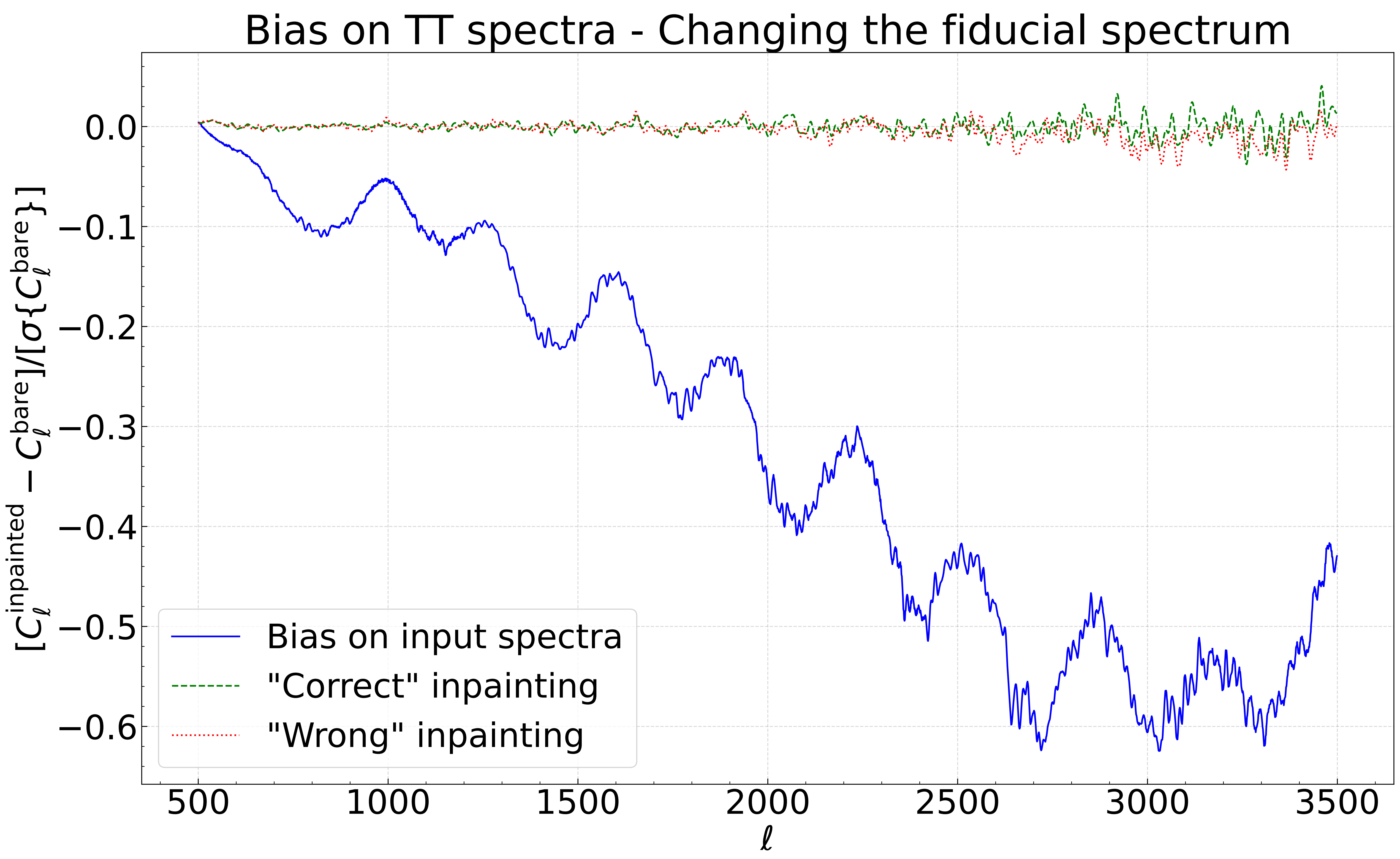

2. Robustness against input spectrum

$$\begin{pmatrix} T^{\mathrm{inp}} \\ Q^{\mathrm{inp}} \\ U^{\mathrm{inp}} \end{pmatrix} = \boxed{X} \begin{pmatrix} T^{\mathrm{data}} \\ Q^{\mathrm{data}} \\ U^{\mathrm{data}} \end{pmatrix} + (1 - \boxed{X}) \boxed{\begin{pmatrix} T^{\mathrm{random}} \\ Q^{\mathrm{random}} \\ U^{\mathrm{random}} \end{pmatrix}}$$

C_ℓ^{fid}

Inpainting requires a fiducial spectrum

We show that we are robust against variations of the input spectrum

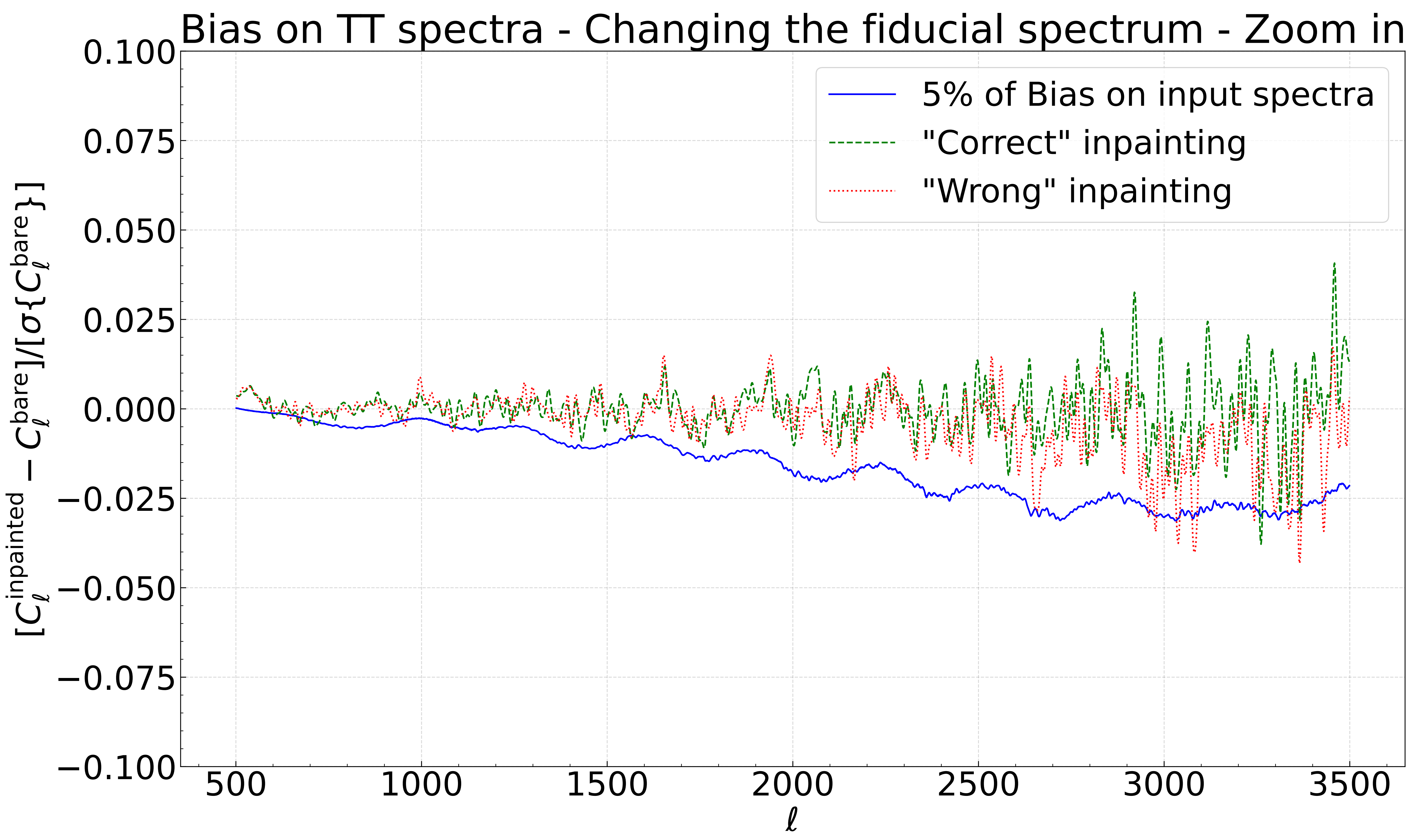

3. Response function

$$\begin{pmatrix} T^{\text{inp}} \\ Q^{\text{inp}} \\ U^{\text{inp}} \end{pmatrix} = \boxed{X} \begin{pmatrix} T^{\text{data}} \\ Q^{\text{data}} \\ U^{\text{data}} \end{pmatrix} + (1 - \boxed{X}) \boxed{\begin{pmatrix} T^{\text{random}} \\ Q^{\text{random}} \\ U^{\text{random}} \end{pmatrix}}$$

C_ℓ^{fid}

Inpainting requires a fiducial spectrum

We show that the response function is negligible

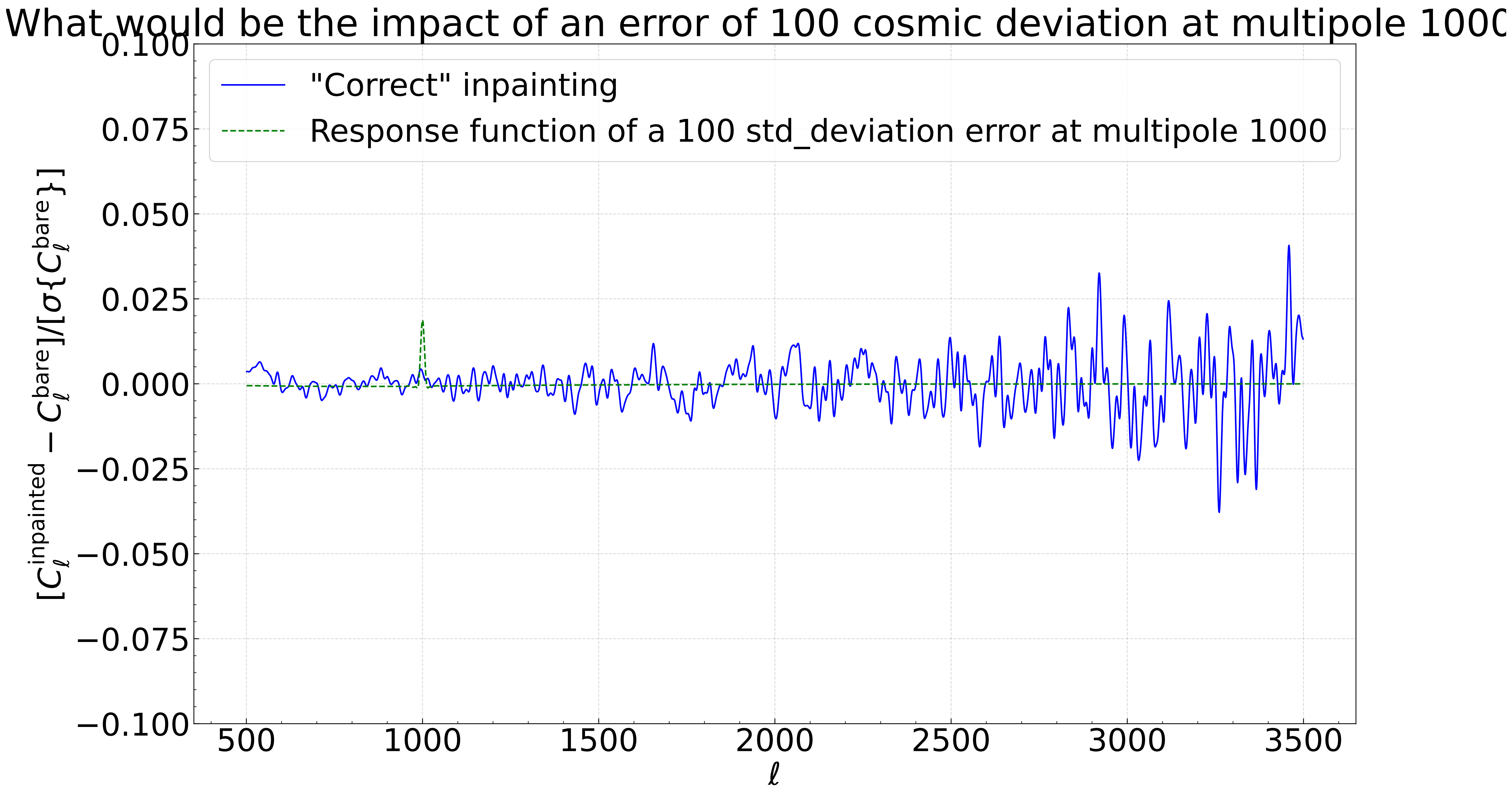

4. Impact on covariance

- We compare the covariance of pure CMB simulations with the covariance of inpainted simulations
- **We show that our inpainting does not create any additional variance or coupling**
- **Our inpainted CMB behaves like a CMB**

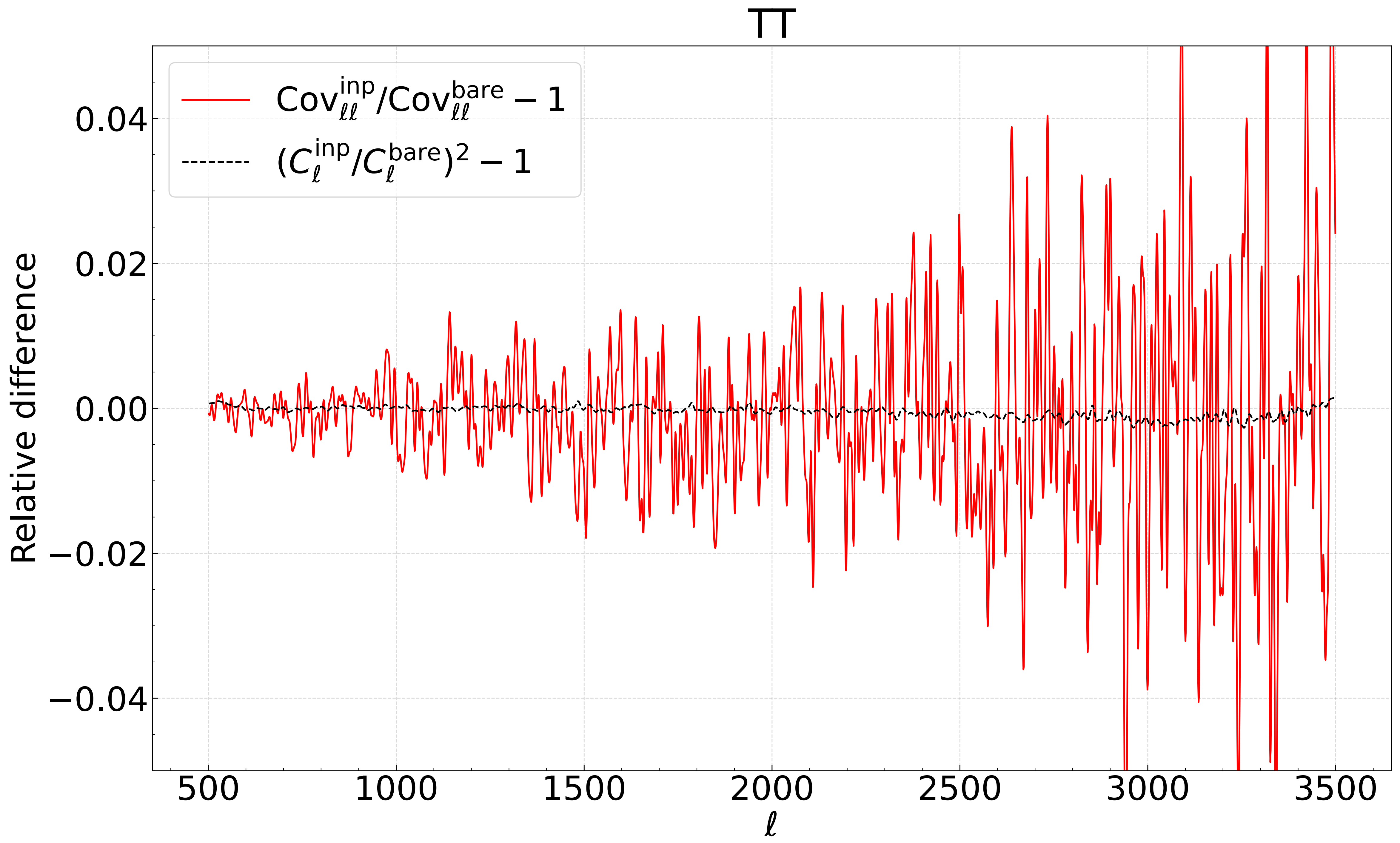

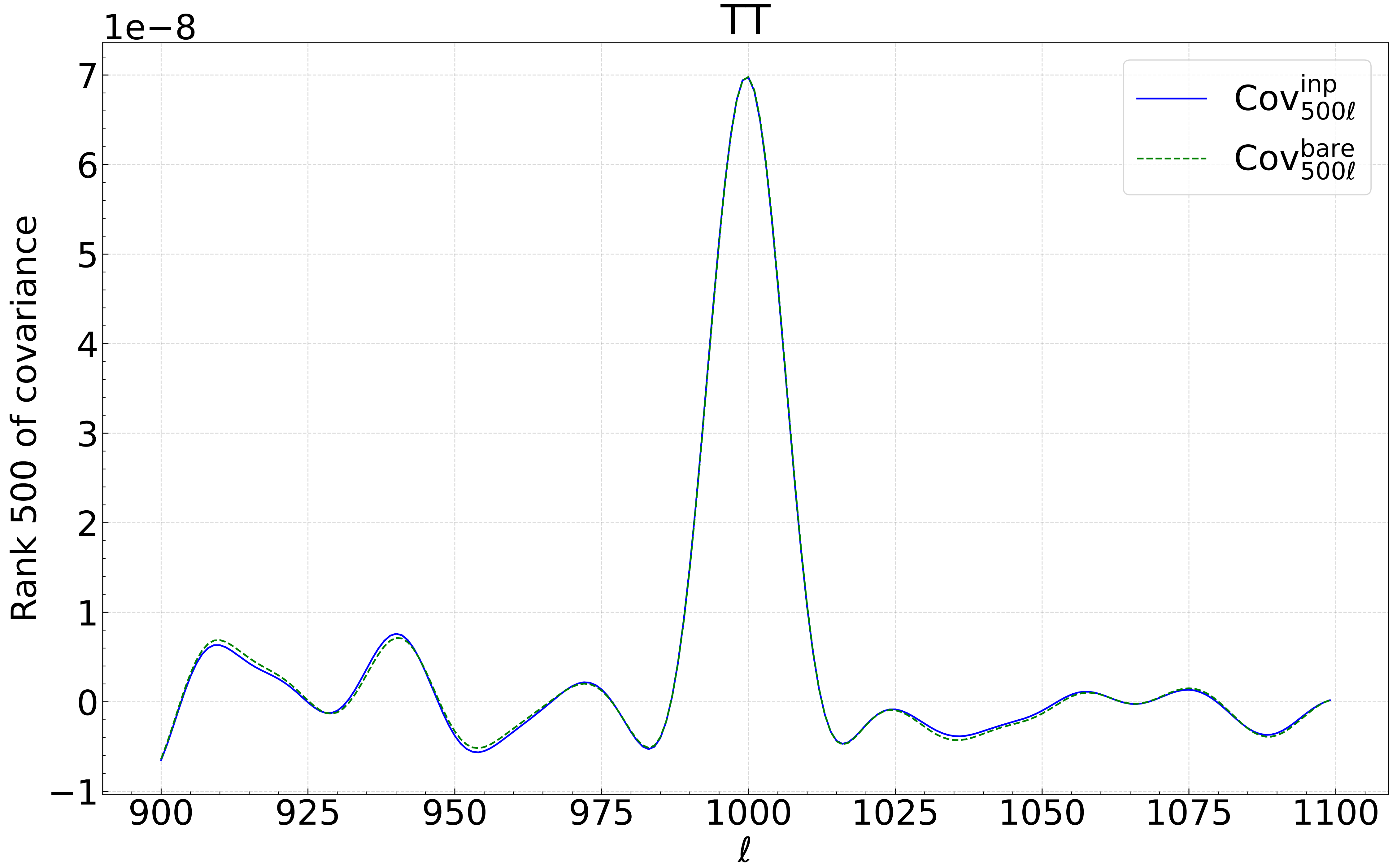

5. Adapting covariance

- Back to inpainting

$$\begin{pmatrix} T^{\mathrm{inp}} \\ Q^{\mathrm{inp}} \\ U^{\mathrm{inp}} \end{pmatrix} = X \begin{pmatrix} T^{\mathrm{data}} \\ Q^{\mathrm{data}} \\ U^{\mathrm{data}} \end{pmatrix} + (1-X) \begin{pmatrix} T^{\mathrm{random}} \\ Q^{\mathrm{random}} \\ U^{\mathrm{random}} \end{pmatrix}$$

Inpainted data

Filtered data

Anti-filtered random realization

- $\langle \hat{C}_\ell^{\mathrm{inp}} \rangle = \langle \hat{C}_\ell^{XD} \rangle + \langle \hat{C}_\ell^{(1-X)R} \rangle = \langle C_\ell^{\mathrm{data}} \rangle$

- **We do not want to use the random realization as true data**

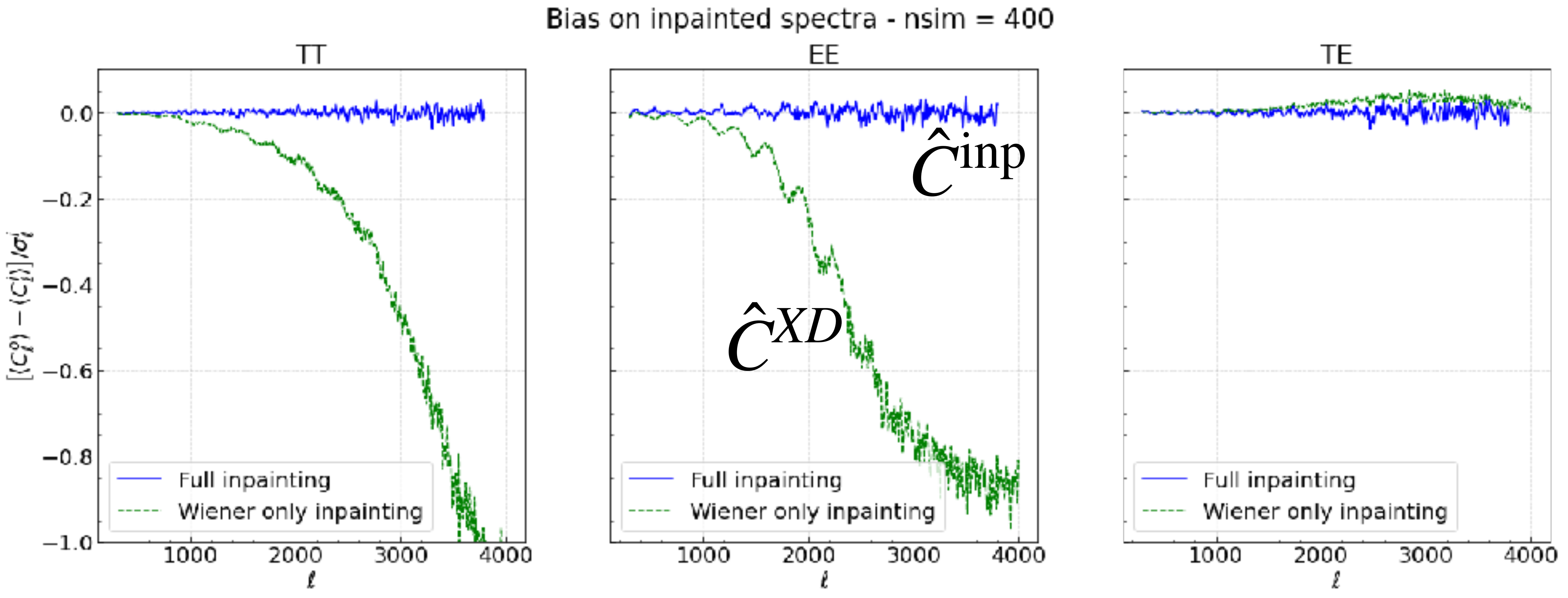

$\rho_\ell = \dfrac{\langle \hat{C}_\ell^{XD} \rangle}{\langle \hat{C}_\ell^{\mathrm{inp}} \rangle}$ gives the contribution of the filtered data in the output spectrum

We can rescale the covariance

$$\Sigma^{\mathrm{inp}} = \frac{1}{\rho} \otimes \frac{1}{\rho} \Sigma^{\mathrm{analytical}}$$

6. Efficiency

- Wiener filtered is obtained analytically

$$\begin{pmatrix} T^{\rm inp} \\ Q^{\rm inp} \\ U^{\rm inp} \end{pmatrix} = \boxed{X} \begin{pmatrix} T^{\rm data} \\ Q^{\rm data} \\ U^{\rm data} \end{pmatrix} + (1 - \boxed{X}) \begin{pmatrix} T^{\rm random} \\ Q^{\rm random} \\ U^{\rm random} \end{pmatrix}$$

Optimal CMB reconstruction
Wiener filtering

- Applying the filter takes most of the CPU-time (because of inversions!)

- Our code is **parallelized**
- **Allows inpainting of multiple maps at the same time** => divide the effective time by the number of maps
- on 64 CPUs: 30 mins per map (for 50 maps) for 2000 sources to inpaint

Credits: Aman Chokshi

Conclusions

- SPT-3G will put tight constraints on parameters
- In order to use our analytical framework for the covariance matrix, we decided to inpaint our maps
- Upcoming work [Camphuis, Benabed et al. in prep]

A. High precision
B. Robust against input spectrum
C. Does not create additional variance or coupling
D. Can be propagated to the covariance

Caveat

Why ?

- The holes in the mask gives $\bar{\Theta}$ an offset
- This will be convoluted with the CMB power spectrum

$$\mathrm{Cov}(\tilde{C}_\ell, \tilde{C}_{\ell'}) = 2\Xi_{\ell\ell'}[W^2] \sum_{\ell_1\ell_2} C^{\mathrm{th}}_{\ell_1}\, \bar{\Theta}^{\ell_1\ell_2}_{\ell\ell'}[W]\, C^{\mathrm{th}}_{\ell_2}$$

- (In the plot, $\bar{\Theta}$s have been renormalized)

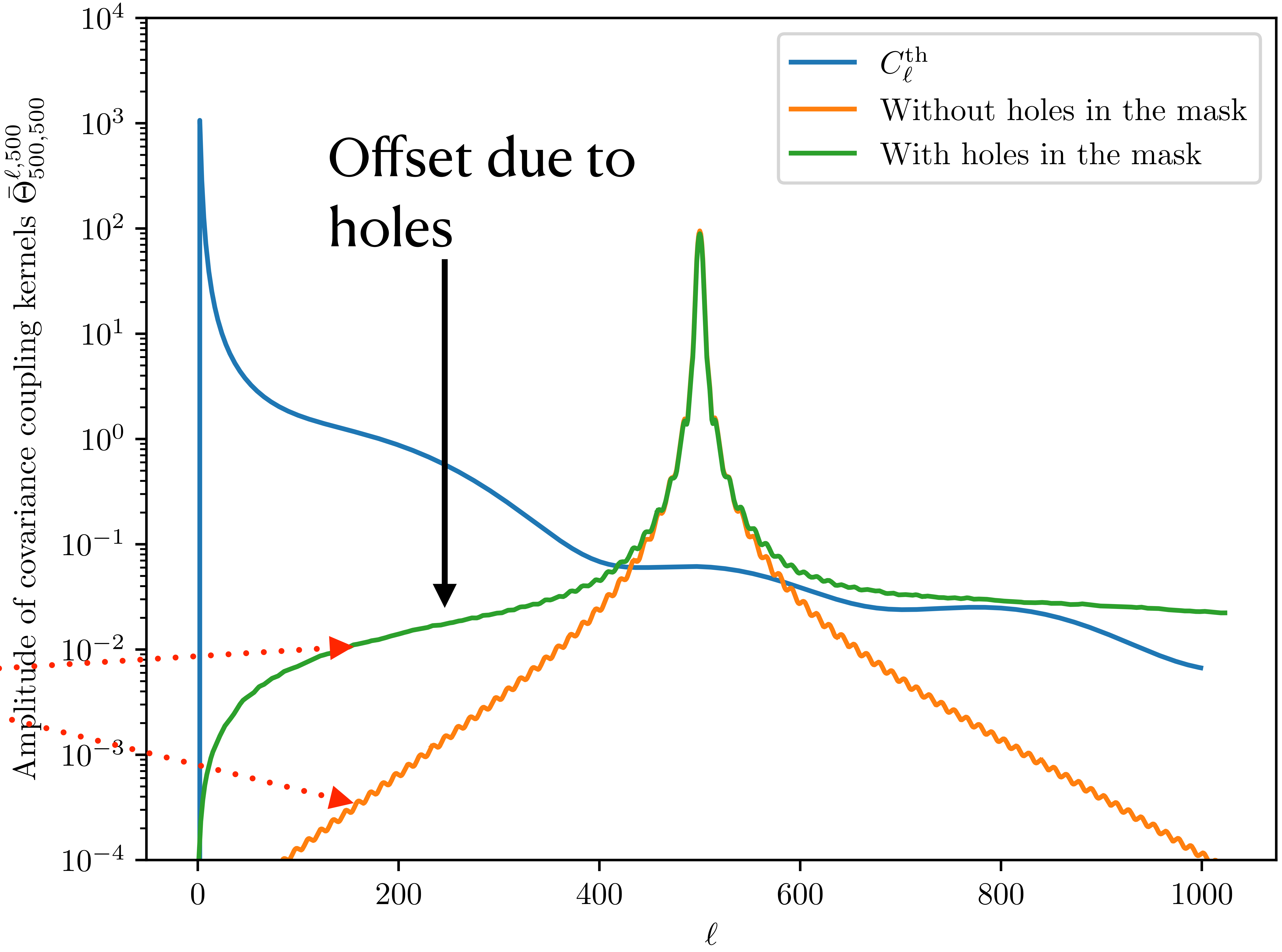

Signal to noise